ENGINEERING RESEARCH INSTITUTE
UNIVERSITY OF MICHIGAN
ANN ARBOR

THEORETICAL STUDY, DESIGN, AND CONSTRUCTION OF C-W MAGNETRONS FOR FREQUENCY MODULATION

QUARTERLY PROGRESS REPORT NO. 2

Period Covering March 1, 1951 to June 1, 1951
Electron Tube Laboratory
Department of Electrical Engineering

BY

H. W. WELCH, JR.

J. R. BLACK
G. R. BREWER
J. S. NEEDLE
S. RUTHBERG
G. HOK
W. PETERSON

Approved by: W. G. DOW

Project M921

CONTRACT NO. DA-36-039 sc-5423
SIGNAL CORPS, DEPARTMENT OF THE ARMY
DEPARTMENT OF ARMY, PROJECT NO. 3-99-13-022
SIGNAL CORPS PROJECT 27-112B-0

June, 1951

TABLE OF CONTENTS

LIST OF FIGURES

LIST OF FIGURES (CONT'D.)

PERSONNEL

Scientific and Engineering Personnel		Time Worked in Man Months*
W. G. Dow	Professor of Electrical Engineering	Supervisor
H. W. Welch, Jr.	Research Physicist	1.35
J. R. Black	Research Engineers	2.18
G. Hok		2.05
J. S. Needle	Instructors in Electrical Engineering	2.17
J. A. Boyd		.39
R. Hegler		.12
G. R. Brewer	Research Associates	1.17
S. Ruthberg		2.18
W. W. Peterson	Student Assistant	1.26
Service Personnel		
V. R. Burris	Machine Shop Foreman	1.63
R. F. Steiner	Assembly Technicians	2.67
J. W. VanNatter		2.92
R. J. Hansen	Technicians	.74
C. A. Jaycox		.94
R. F. Denning	Laboratory Machinists	2.25
D. L. McCormick		.40
T. G. Keith		2.98
E. A. Kayser		.55
N. Navarre	Draftsman	1.97
J. Long	Stenographer	1.25

* Time worked is figured on the basis of 172 hours per month.

MAJOR REPORTS ISSUED TO DATE

Contract No. W-36-039 sc-32245. Subject: Theoretical Study, Design and Construction of C-W Magnetrons for Frequency Modulation.

Technical Report No. 1 --

H. W. Welch, Jr., "Space-Charge Effects and Frequency Characteristics of C-W Magnetrons Relative to the Problem of Frequency Modulation", November 15, 1948.

Technical Report No. 2 --

H. W. Welch, Jr., G. R. Brewer, "Operation of Interdigital Magnetrons in the Zero-Order Mode ", May 23, 1949.

Technical Report No. 3 --

H. W. Welch, Jr., J. R. Black, G. R. Brewer, G. Hok, "Final Report", May 27, 1949.

Contract No. W-36-039 sc-35561. Subject: Theoretical Study, Design and Construction of C-W Magnetrons for Frequency Modulation.

Technical Report No. 4 --

H. W. Welch, Jr., "Effects of Space Charge on Frequency Characteristics of Magnetrons", Proc. I.R.E., 38, 1434-1449, December, 1950.

Technical Report No. 5 --

H. W. Welch, Jr., S. Ruthberg, H. W. Batten, W. Peterson, "Analysis of Dynamic Characteristics of the Magnetron Space Charge, Preliminary Results", January, 1951.

Technical Report No. 6 --

J. S. Needle, G. Hok, "A New Single-Cavity Resonator for a Multianode Magnetron", January 8, 1951.

Technical Report No. 7 --

J. R. Black, H. W. Welch, Jr., G. R. Brewer, J. S. Needle, W. Peterson, "Theoretical Study, Design, and Construction of C-W Magnetrons for Frequency Modulation", Final Report, February, 1951.

QUARTERLY PROGRESS REPORT NO. 2

THEORETICAL STUDY, DESIGN, AND CONSTRUCTION OF C-W MAGNETRONS FOR FREQUENCY MODULATION

1. Objectives for the Period (J. R. Black)

The purpose of this report is to summarize the progress in the University of Michigan Electron Tube Laboratory during the period from March 1, 1951 to June 1, 1951, on Contract No. DA-36-039 sc-5423.

The general objectives of the program under this contract are to increase the knowledge of space-charge effects and frequency characteristics in c-w magnetrons and to apply this knowledge to the development of magnetrons which can be frequency-modulated. Prior to December 1, 1950, the major emphasis has been on the development of an improved understanding of the magnetron space charge and its effects on magnetron modulation and operation. In particular, the magnetron space charge as a reactive element was given rather extensive attention and, more recently, the phenomena of voltage tuning and frequency pushing were studied. As a result of these studies, the development of several tube structures have been started. This development has suffered somewhat because of the emphasis on theoretical study and analysis.

On March 1, there were two primary objectives for the period covered by this report. One was to continue the emphasis on the development of various tube designs into practically usable form. The other was to continue the theoretical aspects of the program with the aim of using the results in the design of new tubes.

The tube designs to be emphasized are the Model 6 and Model 8 f-m magnetrons and the Model 9 magnetron for use in an external tunable cavity at power levels less than one watt. Voltage tuning is to be investigated on all tubes with emphasis on the Model 9. The tubes are all described in detail in Technical Report No. 7, the Final Report on Contract No. W-36-039 sc-35561.

2. Technical Reports (G. R. Brewer)

During the past few years, several articles presenting theoretical considerations on the subject of the magnetron, the proposed magnetron wave tube, electron waves, and plasma waves, have appeared in the foreign periodical literature. A number of these articles were of sufficient interest to the personnel of the Electron Tube Laboratory to warrant translation. These translated articles are listed below, and copies are available upon request.

It is thought that a few of these translated articles would be of interest to other workers in the field, so that those indicated by an asterisk will be made available as technical reports from this project.

*1. O. Doehler, "On the Properties of Tubes in a Constant Magnetic Field -- Part I, Characteristics and Trajectories of the Electrons in the Magnetron", Ann. de Radioélec., 3, No. 11, Jan., 1948, pp 29-39.

*2. O. Doehler, "Part II, The Oscillations of Resonance", Ann. de Radioélec., 3, No. 13, July, 1948, pp 169-183.

*3. O. Doehler and J. Brossart, "Part III, The Travelling-Wave Tube in a Magnetic Field", Ann. de Radioélec., 3, No. 14, Oct., 1948, pp 328-338.

*4. O. Doehler, J. Brossart, G. Mourier, "Part IV, Extension of the Linear Theory, the Effects of Non-Linearities and the Efficiency", Ann. de Radioélec., 5, No. 22, Oct., 1950, pp 293-307.

5. P. Guénard, R. Berterottière, and O. Doehler, "Amplification by Direct Electronic Interaction in Tubes without Circuit", Ann. de Radioélec., 4, 1949, p. 172.

*6. J. Labus, "HF Amplification by Means of the Interchange Effect between Electron Streams", Arch. Elekt. Ubertragung, 4, 1950, p. 353.

*7. W. O. Schumann, "On Electric Waves in a Moving Plasma", Zeits. f. Angew. Physik., II, No. 10, Oct., 1950, p. 28.

8. Karl Forsterling, "The Propagation, with Oblique Incidence, of Electromagnetic Waves in a Stratified Medium under the Influence of a Magnetic Field", Arch. Elekt. Ubertragung, 3, 1949, pp 115-120.

9. I. I. Wasserman, "Rotating Space Charge in a Magnetron with Solid Anode", J. Tech. Phys. (U.S.S.R.), 18, 1948, p. 785.

10. N. S. Zintchenko, "Stability of Magnetron Oscillations of the Dynatron Type", Ratiotekhaika, 3, 1948, pp 40-53.

3. Model 9 Low-Power Insertion Magnetron (J. S. Needle)

The Model 9 series low-power insertion magnetron consists of a multi-anode structure and cathode contained in an evacuated metal and glass envelope. This sealed-off structure serves only as the capacitive part of an external resonator system. The basic structure of this sealed-off insertion magnetron consists of six equally-spaced radial vanes attached to the inner wall of an outer cylinder which protrude through six longitudinal slots in an inner cylinder. The evacuated envelope thus forms a short section of coaxial transmission line coupled to a 12-anode magnetron structure. The interaction space-design parameters for the Model 9 series of magnetrons are listed below:

λ	= 10 cm	E_o	= 280 volts
$n\lambda$	= 60	E	= 1400 volts
n	= N/2 = 6	B_o	= 554 gauss
r_a	= .317 cm	B	= 1662 gauss
r_c	= .190 cm	B/B_o	= 3
r_a/r_c	= 1.66		

The emphasis during this quarterly period has been on voltage-tunable operation with special emphasis on noise reduction. Four new tubes were completed during this period. A list of these tubes is given below along with their significant design characteristics. The assembly drawings for the Model 9B and Model 9C are given in Figs. 3.1 and 3.2, respectively.

Model	No.	Cathode Type	Body Assembly Dwg. No.
9C	48	Oxide	10009C
9B	49	Tungsten helix	10009B
9B	50	Oxide	10009B
9B	53	Conical tungsten helix	10009B

A tunable cavity designated cavity No. 3 was completed and tested in conjunction with Model 9B, No. 43 under pulsed operating conditions. An assembly drawing of cavity No. 3 is shown in Fig. 3.3. Two sets of data were taken, as shown in Figs. 3.4 and 3.5. The wavelength was measured as a function of tuner distance for the conditions where the tube was operated both with and without an external bypass on the cathode line. The mode-jump current was simultaneously measured as a function of tuner position with and without an external bypass in the cathode circuit. The importance of the cathode circuit with respect to the mode boundary in the mechanically tunable system is immediately apparent from Fig. 3.5. Note the direction of wavelength shift caused by the cathode circuit with relation to the change in mode-jump current.

DWG. NO. B

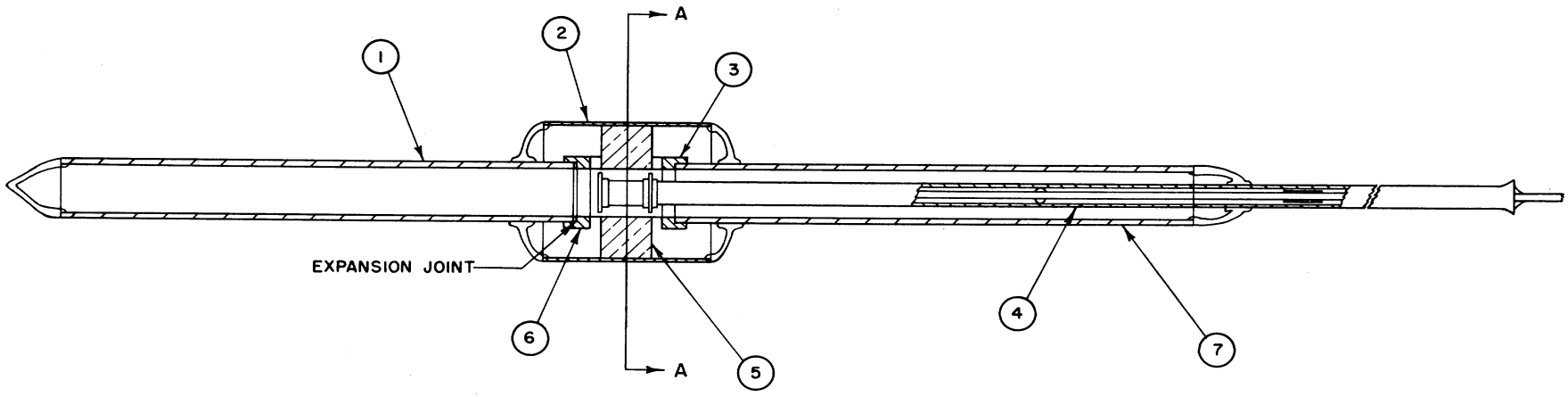

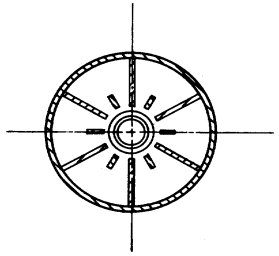

SECTION AA

FIG. 3.1

1/2"

ALL DIMENSIONS UNLESS OTHERWISE SPECIFIED MUST BE HELD TO A TOLERANCE - FRACTIONAL ± 1/64" DECIMAL ± .005" ANGULAR ± 1/2°

ISSUE / DATE	ENGINEERING RESEARCH INSTITUTE UNIVERSITY OF MICHIGAN ANN ARBOR MICHIGAN	DESIGNED BY	APPROVED BY
		DRAWN BY MM	SCALE 2X
		CHECKED BY	DATE 1-22-51
	PROJECT M-921	TITLE LOW POWER MAGNETRON MODEL 9B	
	CLASSIFICATION	DWG. NO. B-10,009 B	

FIG. 3.2

ALL DIMENSIONS UNLESS OTHERWISE SPECIFIED MUST BE HELD TO A TOLERANCE - FRACTIONAL ± 1/64," DECIMAL ± .005," ANGULAR ± ½°

ENGINEERING RESEARCH INSTITUTE
UNIVERSITY OF MICHIGAN
ANN ARBOR MICHIGAN

PROJECT M-921

CLASSIFICATION

ISSUE | DATE

DESIGNED BY JJ
DRAWN BY JJJ
CHECKED BY DRS
APPROVED BY

SCALE 2X
DATE 5-23-51

TITLE
LOW POWER MAGNETRON
MODEL 9C

DWG. NO. B-10,009C

DWG. NO. B

DWG. NO. B

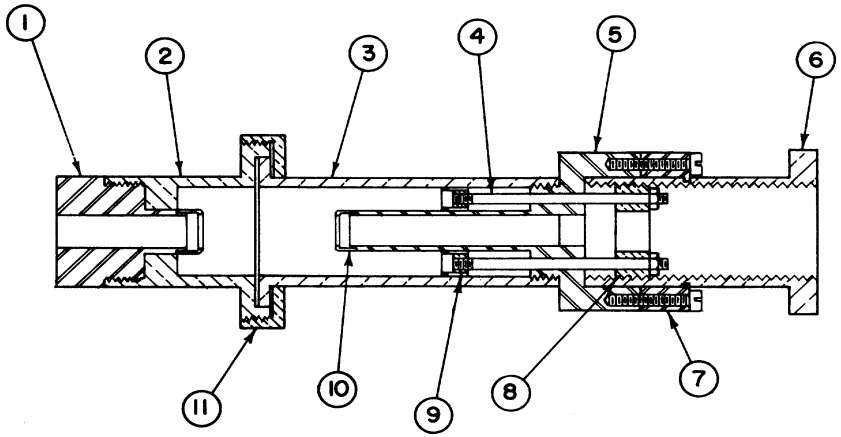

FIG. 3.3

1"

ALL DIMENSIONS UNLESS OTHERWISE SPECIFIED MUST BE HELD TO A TOLERANCE - FRACTIONAL ± 1/64" DECIMAL ± .005" ANGULAR ± 1/2°

		ENGINEERING RESEARCH INSTITUTE UNIVERSITY OF MICHIGAN ANN ARBOR MICHIGAN	DESIGNED BY	APPROVED BY
			DRAWN BY 777	SCALE FULL
			CHECKED BY	DATE 6-7-51
		PROJECT M-921	TITLE CAVITY NO. 3 MOD. 9 MAG.	
ISSUE	DATE	CLASSIFICATION	DWG. NO. B-2053	

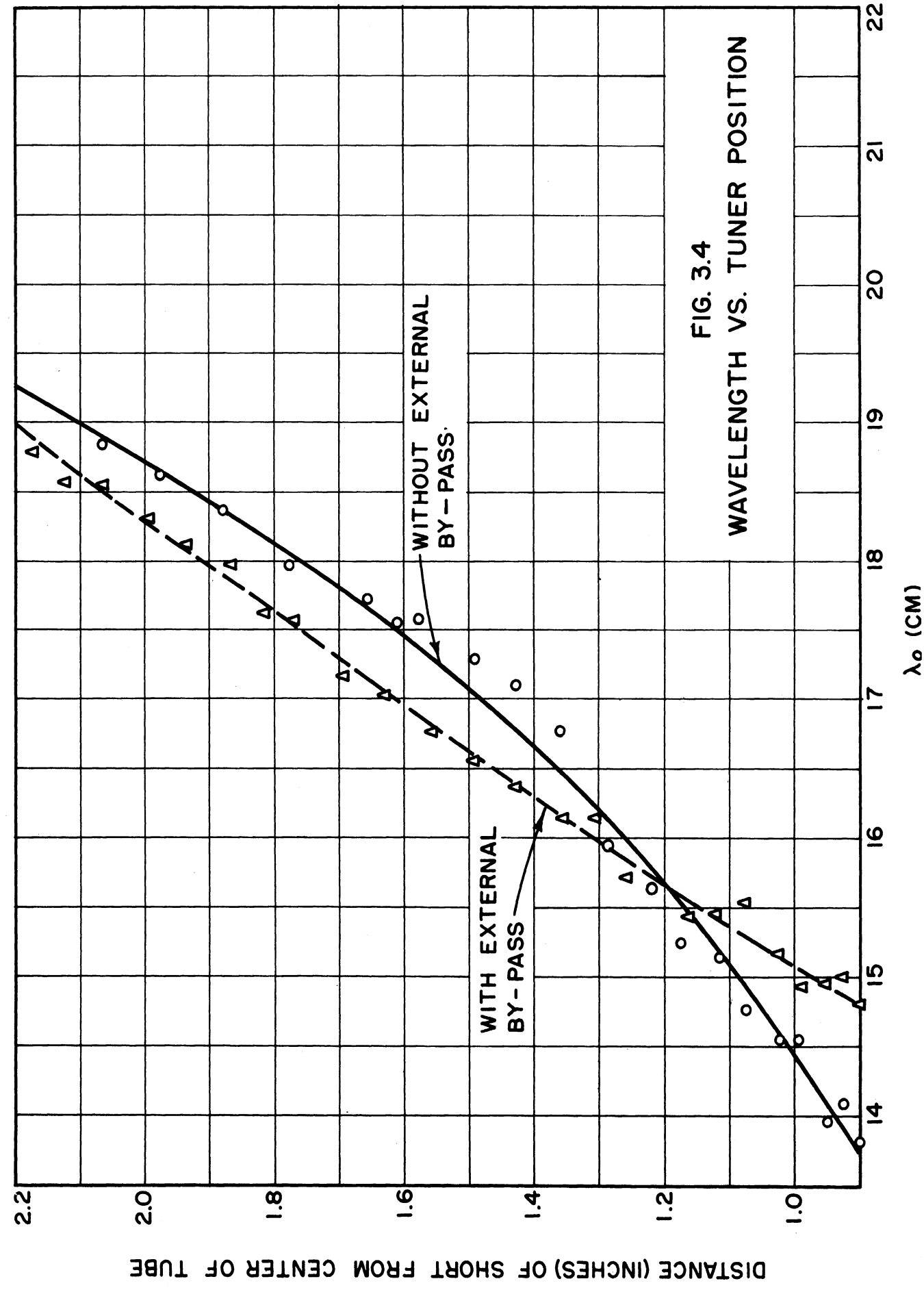
FIG. 3.4
WAVELENGTH VS. TUNER POSITION
WITHOUT EXTERNAL BY-PASS
WITH EXTERNAL BY-PASS
DISTANCE (INCHES) OF SHORT FROM CENTER OF TUBE
λo (CM)
2.2
2.0
1.8
1.6
1.4
1.2
1.0
14
15
16
17
18
19
20
21
22

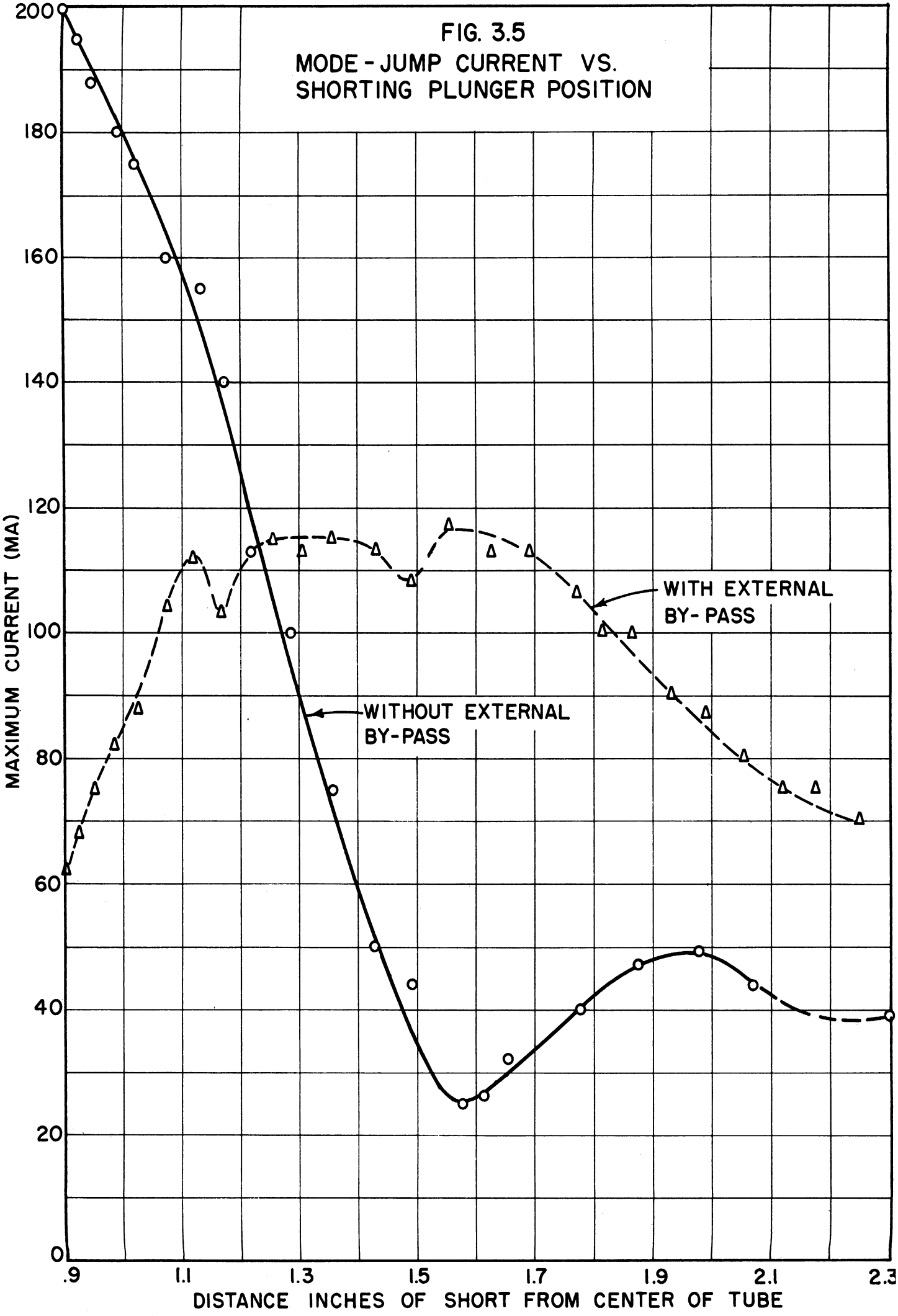
FIG. 3.5
MODE-JUMP CURRENT VS.
SHORTING PLUNGER POSITION
MAXIMUM CURRENT (MA)
200
180
160
140
120
100
80
60
40
20
0
.9
1.1
1.3
1.5
1.7
1.9
2.1
2.3
DISTANCE INCHES OF SHORT FROM CENTER OF TUBE
WITH EXTERNAL BY-PASS
WITHOUT EXTERNAL BY-PASS

In order to study the voltage-tunable characteristics of the insertion tube, it was found convenient to employ the tube as the local oscillator ina spectrum analyzer. The experimental setup is shown in Fig. 3.6. The tube employed was the Model 9B, No. 49, which has a pure tungsten, single-helix cathode, thus permitting temperature-limited operation.

Cavity No. 2, shown in Fig. 3.7, was employed in conjunction with the insertion tube for this experiment. The important results obtained from this operation are shown in Fig. 3.8a and Fig. 3.8b. Fig. 3.8a is a picture of output versus the frequency. The distance between the two vertical pips corresponds to twice the intermediate frequency of the spectrum analyzer or 40 megacycles. The frequencies corresponding to the upper scope trace are 1690 $\pm$ 20 mc. The lower scope trace pips correspond to 2042 $\pm$ 20 mc. The total frequency swing of the frequency-modulated local oscillator was therefore 392 mc under these conditions.

Fig. 3.8b shows the output of the local oscillator versus frequency in the upper trace. An approximate figure for the total frequency swing can be estimated from the distance between the vertical pips, which corresponds to 40 mc. The center frequency for the two tall pips is 1680 mc.

Fig. 3.8c shows the output of the local oscillator as a function of frequency and vividly demonstrates the long-line effect. The upper trace differs from the lower one only in that here the temperature of the filament is slightly lower. The long-line effect promises to be one of the very serious problems which will need attention if voltage-tunable operation is to be practical over a large frequency range.

Fig. 3.8d shows local oscillator output versus frequency at a higher filament temperature than in the previous experiments. The upper oscillograph

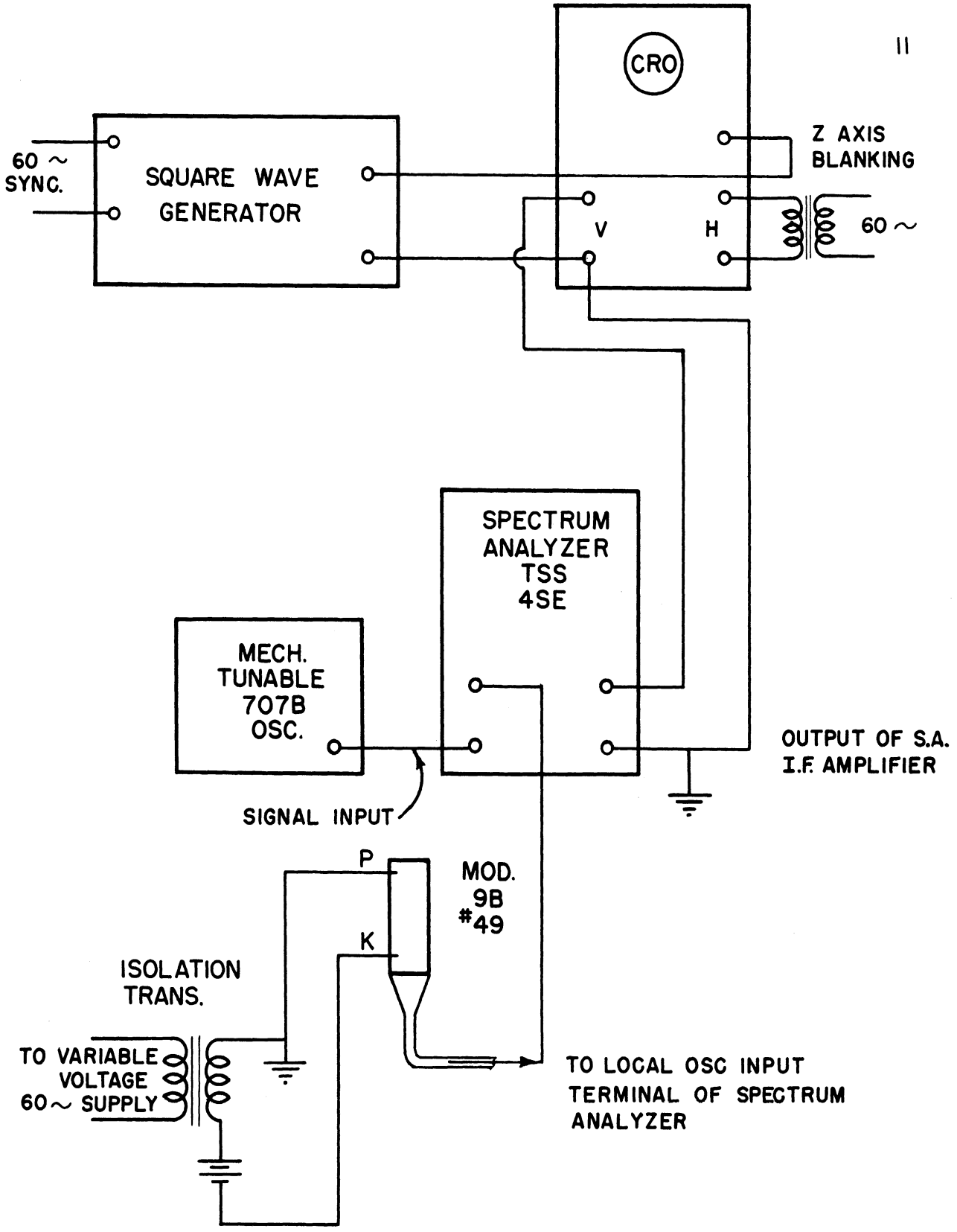

FIG. 3.6

EXPERIMENTAL SET UP USING INSERTION TUBE AS LOCAL OSCILLATOR FOR SPECTRUM ANALYZER.

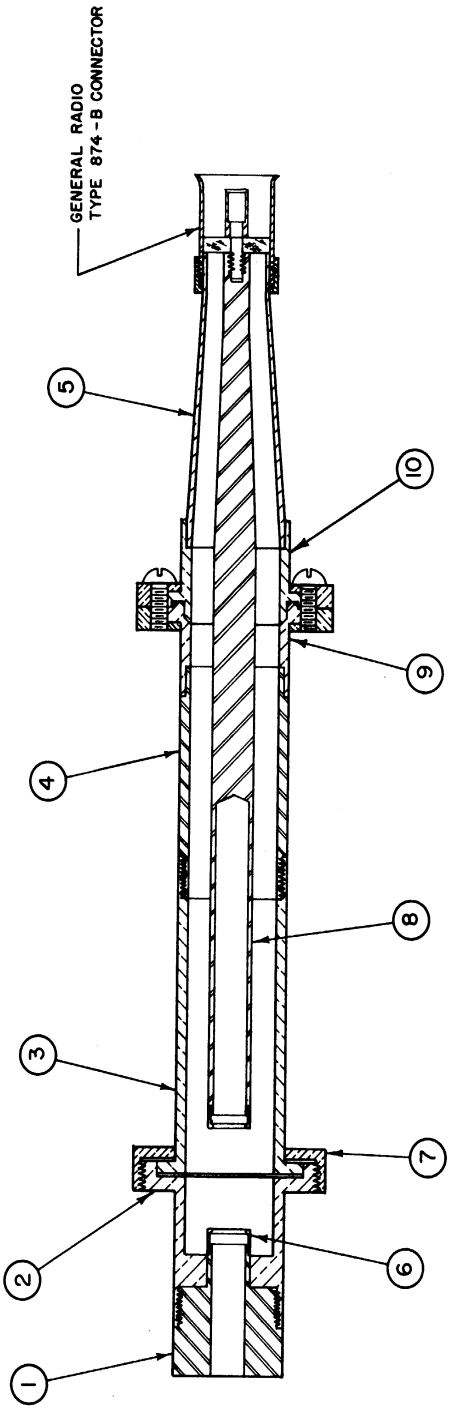

FIG. 3.7

1"

ALL DIMENSIONS UNLESS OTHERWISE SPECIFIED MUST BE HELD TO A TOLERANCE - FRACTIONAL ± 1/32" DECIMAL ± .005" ANGULAR ± 1/2°

ISSUE	DATE

ENGINEERING RESEARCH INSTITUTE
UNIVERSITY OF MICHIGAN
ANN ARBOR MICHIGAN

PROJECT M-921

CLASSIFICATION

DESIGNED BY V. S. N.
DRAWN BY [illegible]
CHECKED BY [illegible]
APPROVED BY
SCALE FULL
DATE 3-16-51

TITLE CAVITY NO. 2, MOD. 9 MAG.

DWG. NO. B-2052

DWG. NO. B

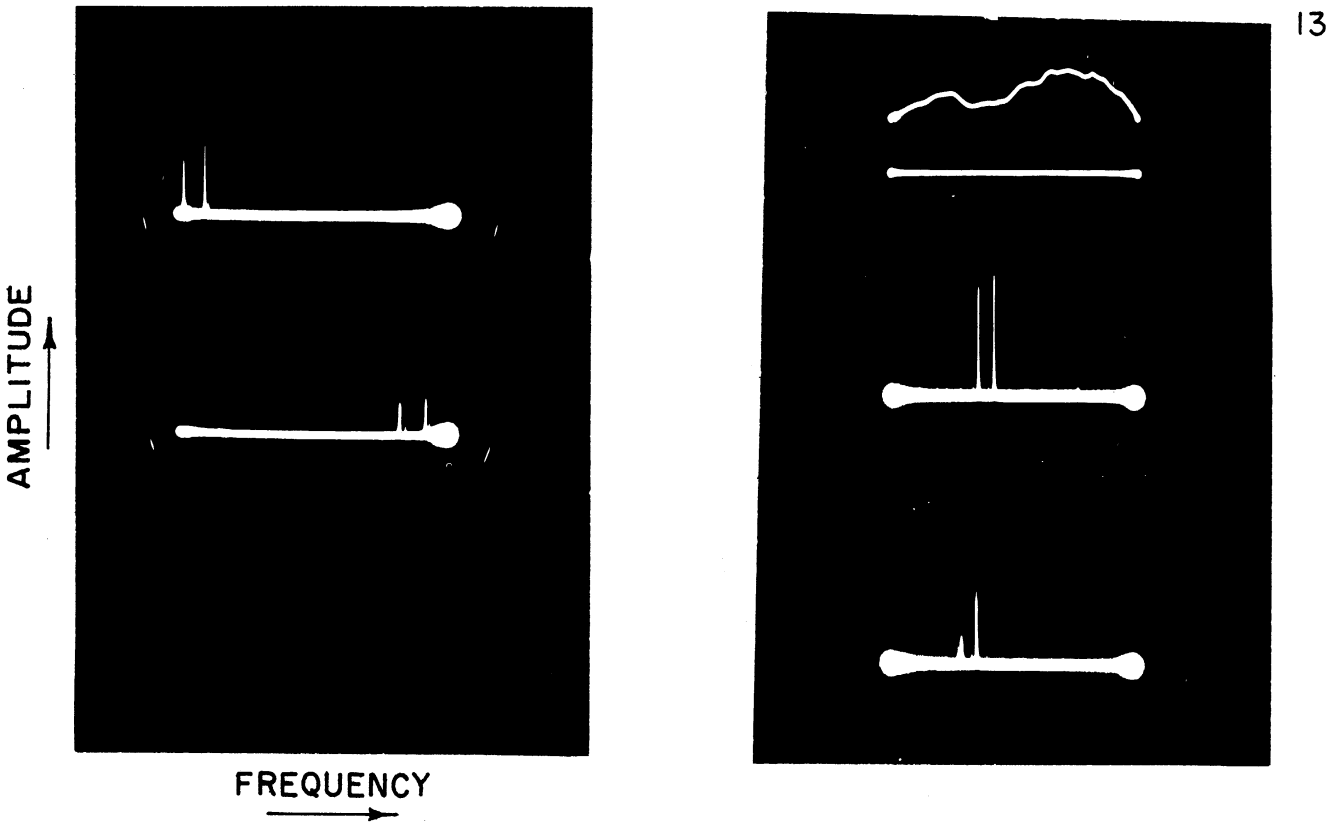

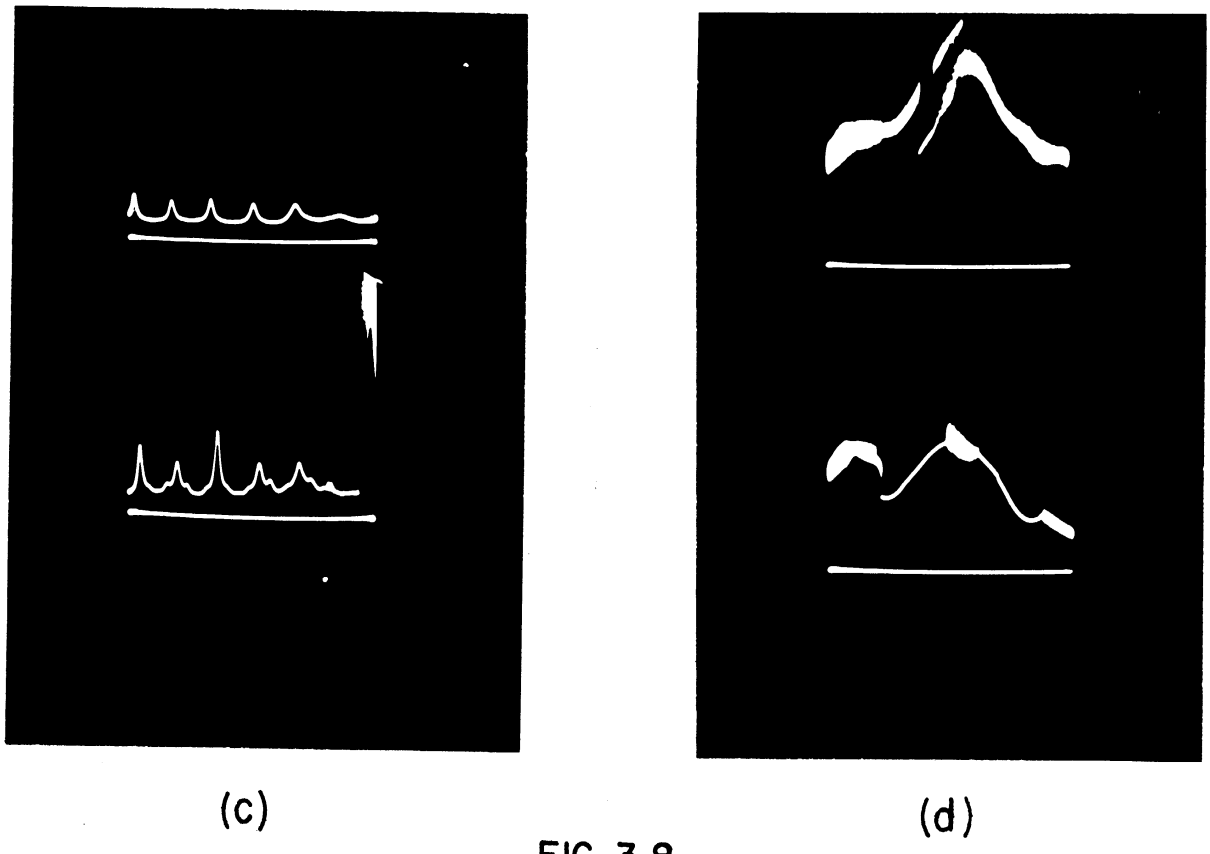

FIG. 3.8

OSCILLOGRAPH TRACES OBTAINED WITH THE EXPERIMENTAL SET UP OF FIG. 3.6

trace in this figure corresponds to a normal magnetic-field configuration. The lower trace was obtained by upsetting the orientation of magnetic field with an iron rod external to the cavity.

Voltage-tunable power output with noise-free operation has so far been of the order of 10 to 400 microwatts. Larger power outputs (up to 3 watts) have been obtained with mechanically tunable cavities; however, the noise has been quite large even under these conditions of higher Q operation.

Work on the Model 9 series will continue with emphasis on increase in noise-free power output. The problems arising from long-line effect will be investigated simultaneously.

4. Model 8 Double-Anode Set Interdigital Magnetron (J. R. Black)

The geometry of the resonant structure of the Model 8 magnetron provides a flexible structure for designing magnetrons for various uses. This is due to the fact that the r-f field distribution within this structure is such that it may be easily affected by external means.

Initially, an effort is being made to adapt the Model 8 structure to an f-m magnetron, as shown in Fig. 4.1b. One set of anodes with its associated cathode will form the magnetron oscillator section, while the other set of anodes with its associated cathode will form a reactance tube employing a magnetron-type space charge as the variable reactance.

To determine the characteristics of the Model 8 structure a high-power tube, as shown in Fig. 4.1a, is being studied. This arrangement employs two oscillator anode sets with their associated cathodes operating in a push-pull type operation. It is believed that over 1000 watts c-w will be obtained from this structure operating at 2300 mc.

An easily tunable magnetron could be built, as shown in Fig. 4.1c. One set of interdigital anodes would form the magnetron oscillator while a

FIG. 4.1

POSSIBLE TYPES OF MAGNETRONS EMPLOYING THE MODEL 8 RESONANT SYSTEM

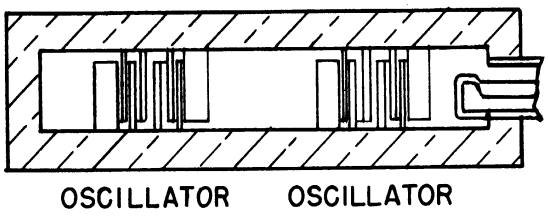

A

HIGH POWER MAGNETRON

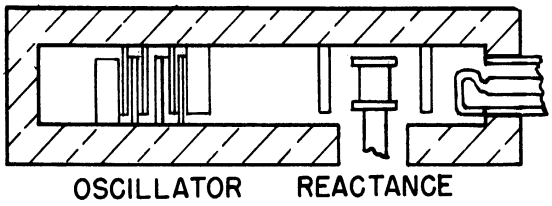

B

F-M MAGNETRON

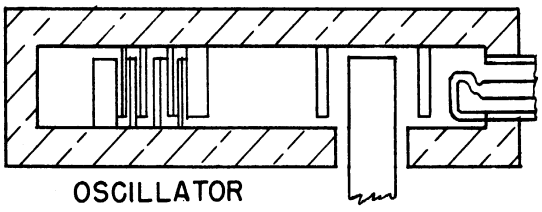

C

TUNABLE MAGNETRON

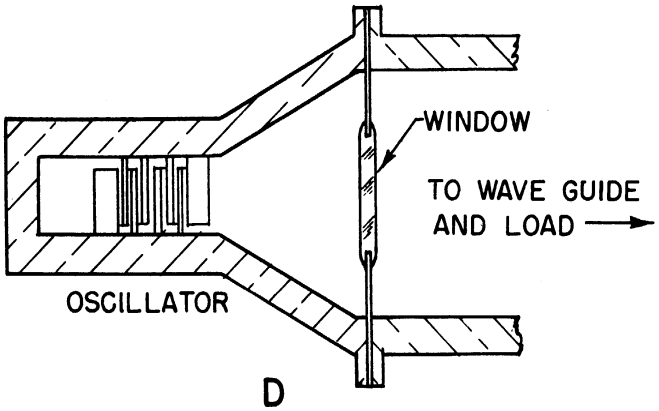

D

VOLTAGE TUNABLE MAGNETRON

mechanically variable condenser would be placed at the other voltage maxima position. As shown below, a simple cup-and-rod variable condenser on cold tests indicated a tuning range in the order of 1.5 to 1 and had no observable parasitic resonances.

A fourth type of use for this structure is indicated in Fig. 4.1d. This system is a means of loading down a magnetron structure having no resonant circuit for use as a voltage-tunable magnetron having an output power in the order of hundreds of watts. One-half of the Model 8 structure would be used feeding directly into a wave guide through a window. See Section 3 of this report for further discussion of voltage tuning.

By enlarging the resonant cavity to include three half-waves down its length a combination of Figs. 4.1b and 4.1c would form a tunable f-m magnetron.

The work to date has been concentrated on the development of a high-power double-anode set magnetron. It is felt that this structure will lead to results immediately applicable to developing an f-m magnetron. At this writing, parts for this tube have been machined and are being cold-tested prior to brazing.

The cavity for this tube (Model 8B), having the dimensions 2.12 x 4.24 cm by 1.016-cm high and containing two sets of anodes with a capacity of approximately 6 $\mu\mu$f each, resonated in the following modes:

$\lambda/2$ mode = 15.22 cm

λ desired mode = 13.20 cm

2λ mode = 9.58 cm

Fig. 4.2 shows the assembly drawing of Model 8B. Two carburized thoriated tungsten cathodes, to be employed in this tube, have been assembled

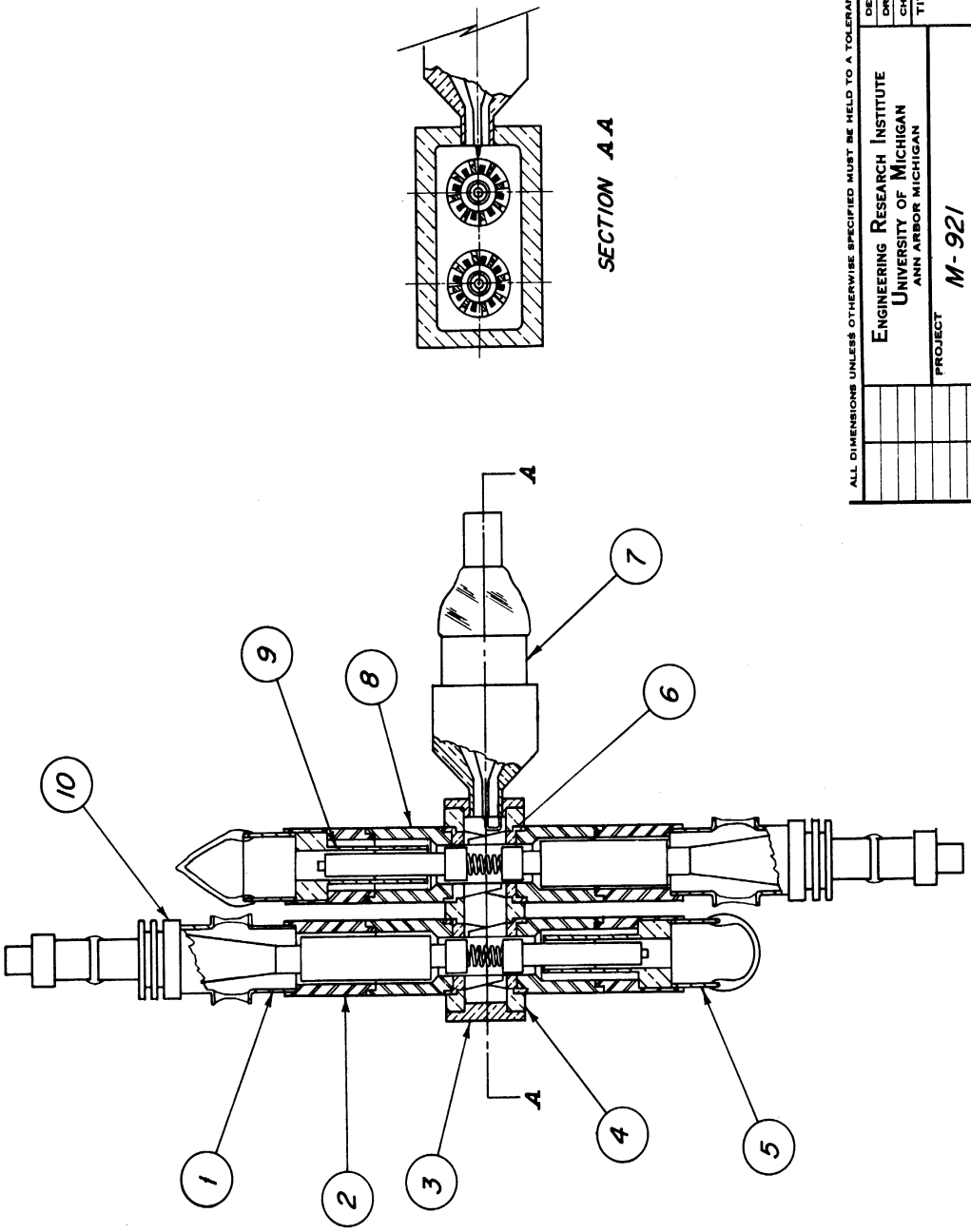

SECTION A-A

FIG. 4.2

ALL DIMENSIONS UNLESS OTHERWISE SPECIFIED MUST BE HELD TO A TOLERANCE - FRACTIONAL ± 1/64" DECIMAL ± .005" ANGULAR ± 1/2°

ENGINEERING RESEARCH INSTITUTE
UNIVERSITY OF MICHIGAN
ANN ARBOR MICHIGAN

PROJECT M-921

CLASSIFICATION

ISSUE | DATE

DESIGNED BY

DRAWN BY

CHECKED BY

APPROVED BY

SCALE FULL

DATE 6-12-51

TITLE PUSH-PULL MAGNETRON MODEL 8B

DWG. NO. B- 10,0088

B DWG. NO.

and tested. Four amperes of diode current were obtained from each cathode. The design factors for Model 8B are as follows:

N	= 16	E_o	= 175 volts
r_a	= .450 cm	B	= 1920 gauss
r_c	= .269 cm	E	= 1925 volts
$r_a r_c$	= 1.67	η_e	= 91 per cent
B_o	= 320 gauss	cavity	= 2.12 x 4.24 cm
		h	= 1.016 cm cavity height

Fig. 4.3 shows a tuning curve obtained from cold tests for Model 8B geometry employing a simple cup-rod variable condenser in place of one of the anode sets. The dimensions for the condenser are given in the insert of this figure. No spurious resonances in the tuning mechanism were noticed; however, as it is tuned to the high-frequency end the desired λ mode produces a voltage node passing through the oscillator anode. This effect undoubtedly will cause a lowering of power output and of efficiency. Oscillations will probably be maintained under this condition since the voltage pattern about the anode is similar to the standard first-order mode found in an ordinary interdigital magnetron.

Fig. 4.3 indicates that if this structure were to be used as an f-m magnetron, 100-mc frequency shift would be obtained per $\mu\mu$f change in capacitance at the reactance tube. The anode for such a reactance tube could be a simple cup eliminating the possibility of oscillations occurring in this section. Capacitance changes in the order of 2 or 3 $\mu\mu$f are to be expected, barring any unforeseen difficulties arising from the high r-f voltages.

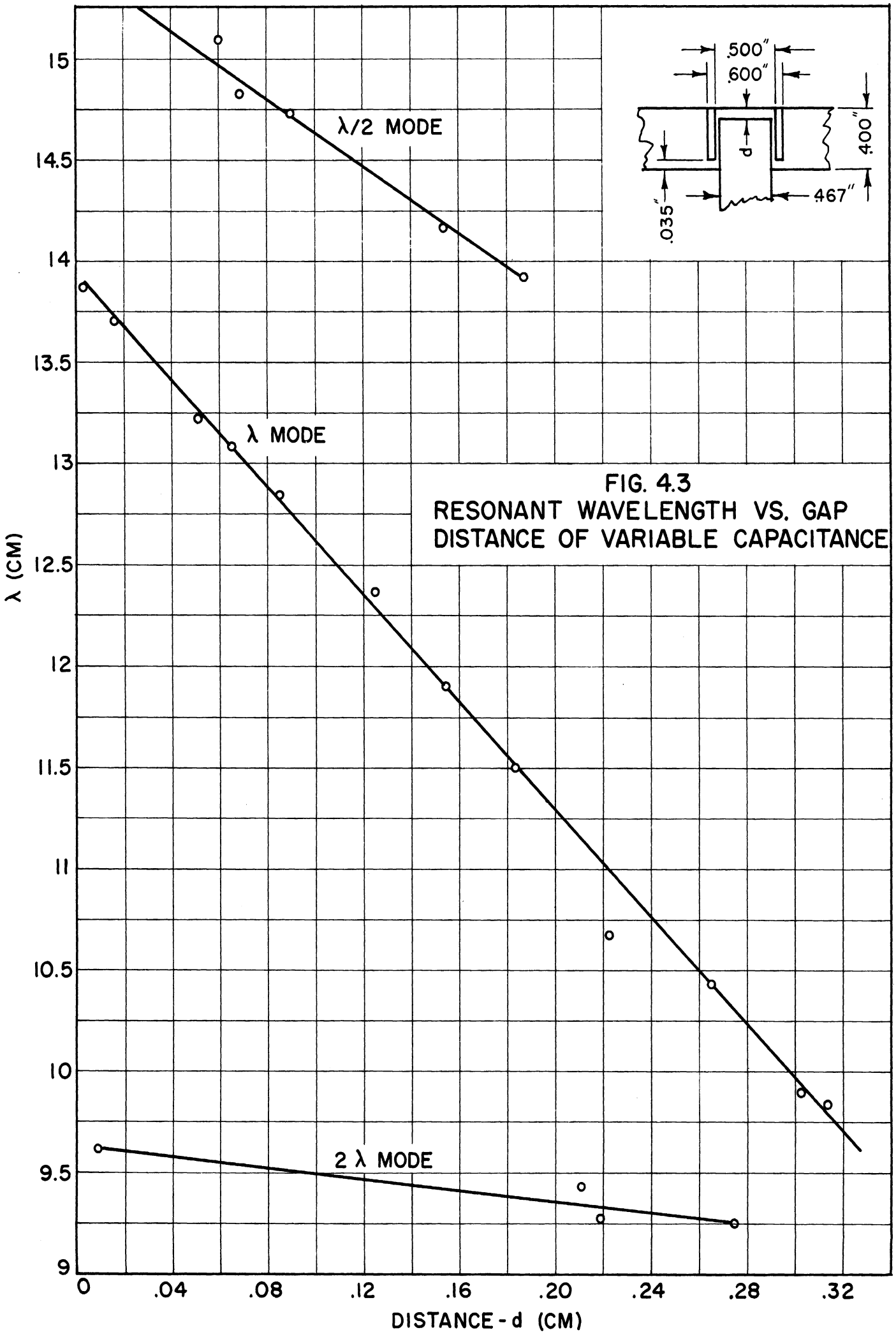

FIG. 4.3
RESONANT WAVELENGTH VS. GAP DISTANCE OF VARIABLE CAPACITANCE

5. Model 6 F-M Magnetron (S. Ruthberg)

The Model 6 f-m magnetron has a coaxial resonant system, two anode sets, and two cathodes. The cavity is electrically one wavelength long for the desired mode of oscillation (λ = 13 cm). Voltage maxima appear at each anode set. The oscillator section consists of 16 anodes and the modulator section has 4 anodes. An assembly drawing of this tube is given in the Appendix of Technical Report No. 7, issued February, 1951.

Eight Model 6 tubes have been constructed, all of which coupled power out of the modulator cathode line. Output power as high as 190 watts at 40 per cent efficiency has been obtained with the modulator cathode removed.

Problems concerning power leakage down the cathode, mode-jump current, etc., are being investigated using a less complicated structure, Model 7, which has an oscillator section identical to the Model 6. The Model 7 coaxial cavity resonator is electrically one-half wavelength long and has no provision for frequency modulation.

The oscillator section of the Model 6 f-m magnetron, which is identical to the Model 7 oscillator, has been receiving consideration. Attention has been given to the optimum operating characteristics, in particular the input impedance of the r-f circuit presented to the interaction space.

As a step in this program, a mechanically tunable Model 7 tube is under construction (designated 7-F); a drawing of which is presented in Fig. 5.1. With this model the operating characteristics may be studied as a function of frequency over a range of .1 cm in the 14-cm wavelength region. The vane, bar, and cathode geometries are those of the Model 7B, which has a single output loop, and a backing ring on the vanes to reduce the vane-mode wavelength. The ratio of anode-to-cathode radius is 2.1. In addition, the cathode-line structure has been modified for better heat transfer.

DWG. NO. B

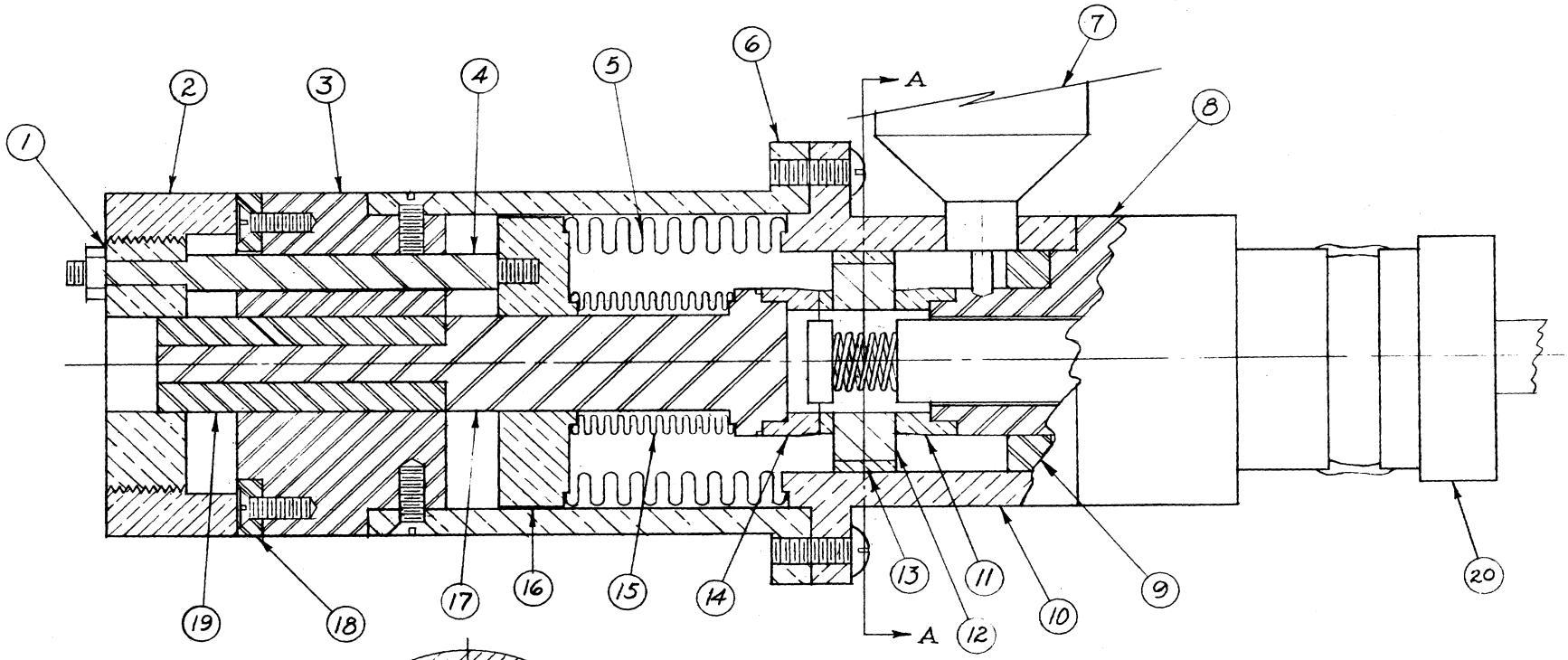

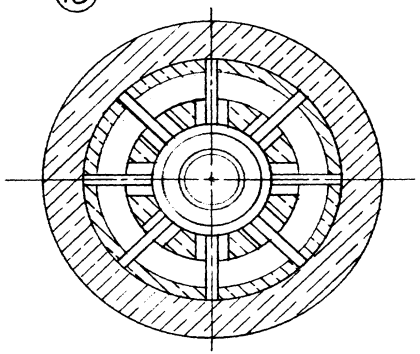

SECTION AA

FIG. 5.1

ALL DIMENSIONS UNLESS OTHERWISE SPECIFIED MUST BE HELD TO A TOLERANCE - FRACTIONAL ± 1/64" DECIMAL ± .005" ANGULAR ± ½°

ENGINEERING RESEARCH INSTITUTE UNIVERSITY OF MICHIGAN ANN ARBOR MICHIGAN		DESIGNED BY	APPROVED BY
		DRAWN BY MM	SCALE 2X
		CHECKED BY	DATE 6-6-51
PROJECT M-921		TITLE TUNABLE CO-AXIAL MAGNETRON MOD. 7F	
CLASSIFICATION		DWG. NO. B-10,007 F	
ISSUE	DATE		

Fig. 5.2 is a photograph of an experimentally obtained magnetic-field flux map of this tube. This shows that a fair amount of distortion exists near the hollow, fixed pole piece. Values of flux density as a function of magnetic-field current are given in Fig. 5.3 for a point midway between the pole faces and on the axis of symmetry. Fig. 5.4 shows the rapid variation of flux density with distance from the axis of symmetry. From such measurements, the average B, in the region of the interaction space on a line 0.775 cm from the fixed pole piece, is indicated as a function of magnetic-field current, I, by the lower curve of Fig. 5.3. These values were taken with a rotating coil fluxmeter, in which the coil is 1/8-in. long by 3 mm in width.

The Model 7E magnetron has been operated c-w. This tube has a modified vane-and-bar structure for the purpose of equalizing the r-f voltage between the cathode and the anode segments by balancing the capacitance between the bars and cathode with that between the vanes and cathode. This geometry is given in Fig. 5.5. The cathode, Fig. 5.6, is oxide-coated, and it has no filter for preventing power loss down the cathode line. Fig. 5.7 lists two representative volt-ampere characteristics. Because of back-heating difficulties, the tube was not operated at much more than 100 watts input power. Both examples given are for a magnetic-field density less than that of the cyclotron frequency but for two different cathode-heater currents. Higher heater power and stronger magnetic fields lead quickly to large back heating. Information about the various modes found in the volt-ampere characteristics may be obtained by use of the Hartree equation and the actual starting voltage. Pulsed operation indicates a greater number of modes than appear in c-w operation. This data will be available in the near future.

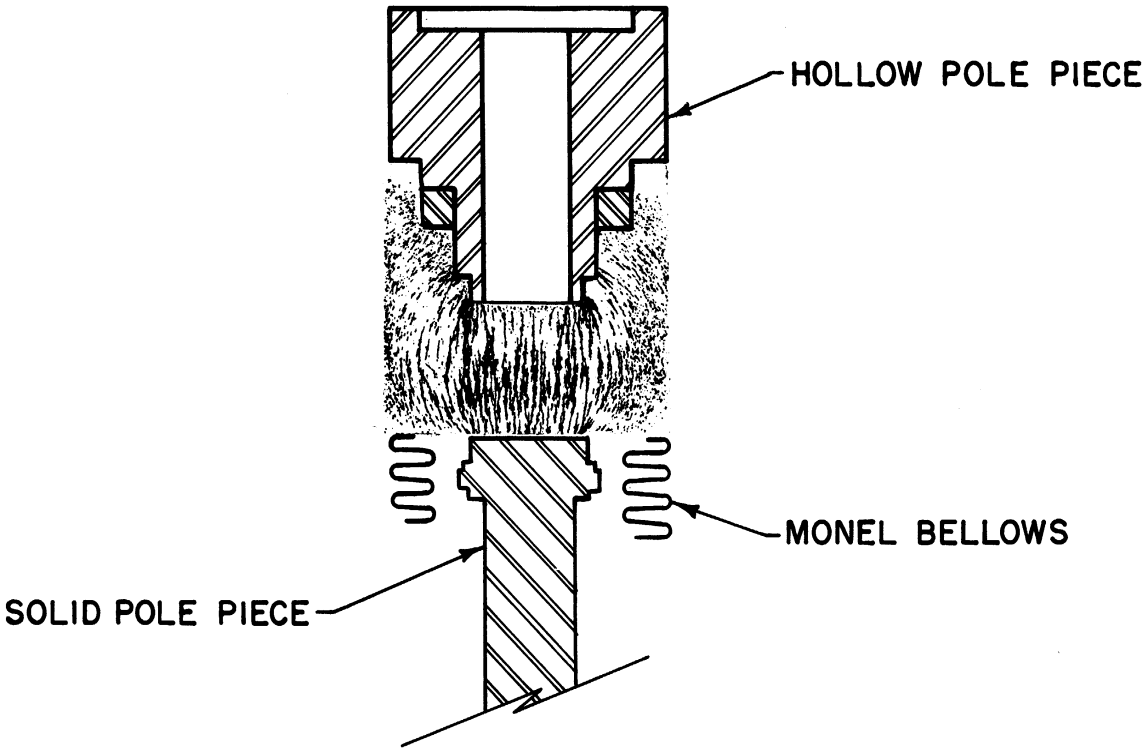

FIG. 5.2
MAGNETIC FIELD FLUX MAP FOR MODEL 7F

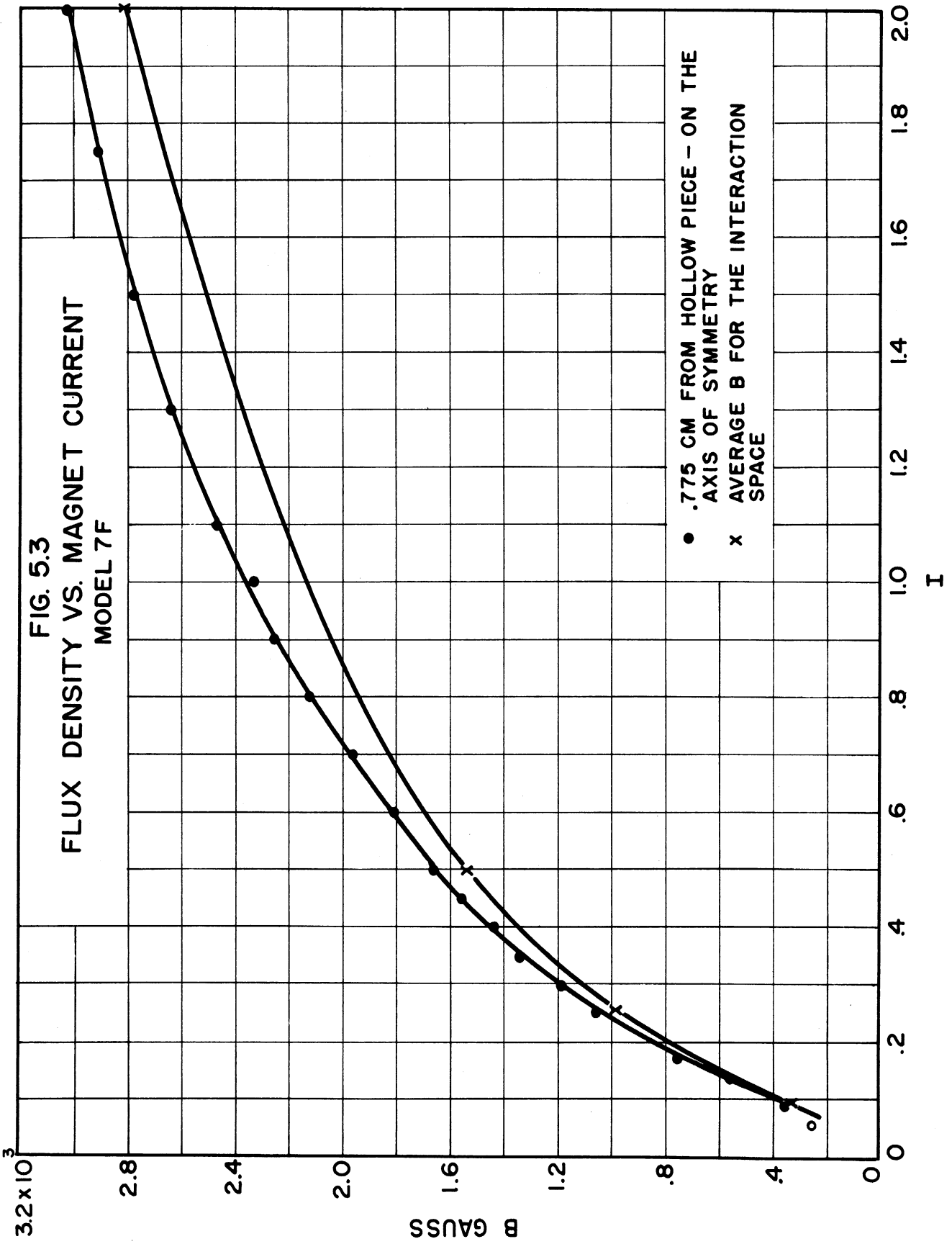
FIG. 5.3
FLUX DENSITY VS. MAGNET CURRENT
MODEL 7F
• .775 CM FROM HOLLOW PIECE – ON THE AXIS OF SYMMETRY
x AVERAGE B FOR THE INTERACTION SPACE
B GAUSS
3.2x10^3
2.8
2.4
2.0
1.6
1.2
.8
.4
0
I
0
.2
.4
.6
.8
1.0
1.2
1.4
1.6
1.8
2.0

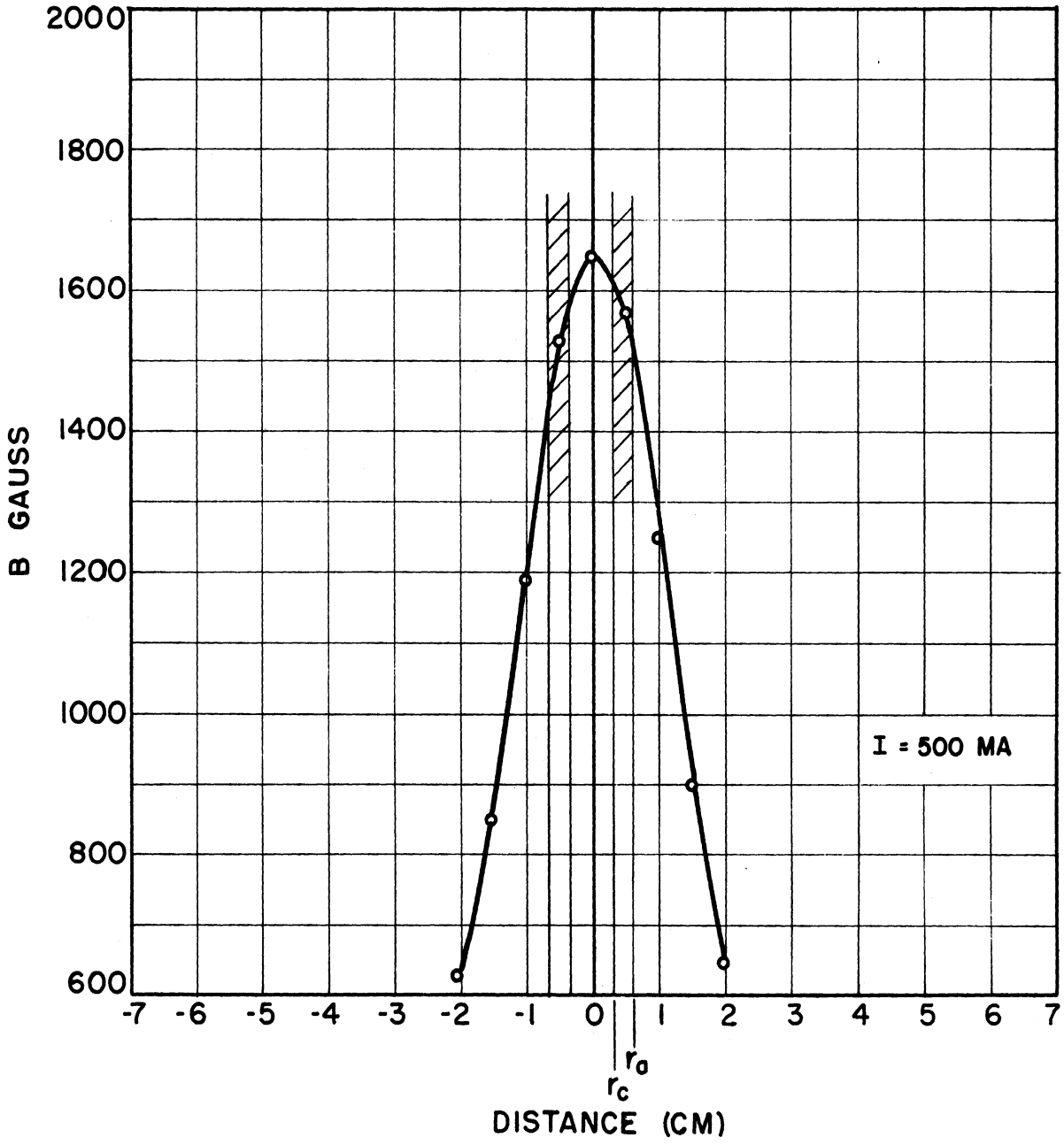

FIG. 5.4

FLUX DENSITY VS. DISTANCE FROM AXIS: MODEL 7F AT .775 CM FROM HOLLOW POLE PIECE

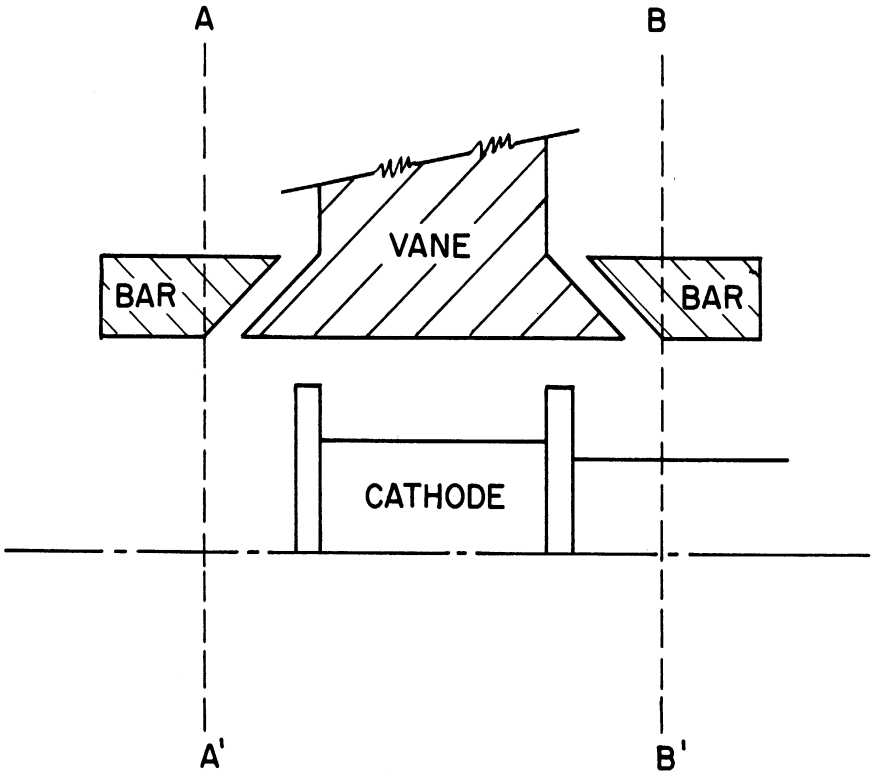

FIG. 5.5

VIEW SHOWING VANE PROTRUDING THROUGH SLOT. MODEL 7E

DWG. NO. A

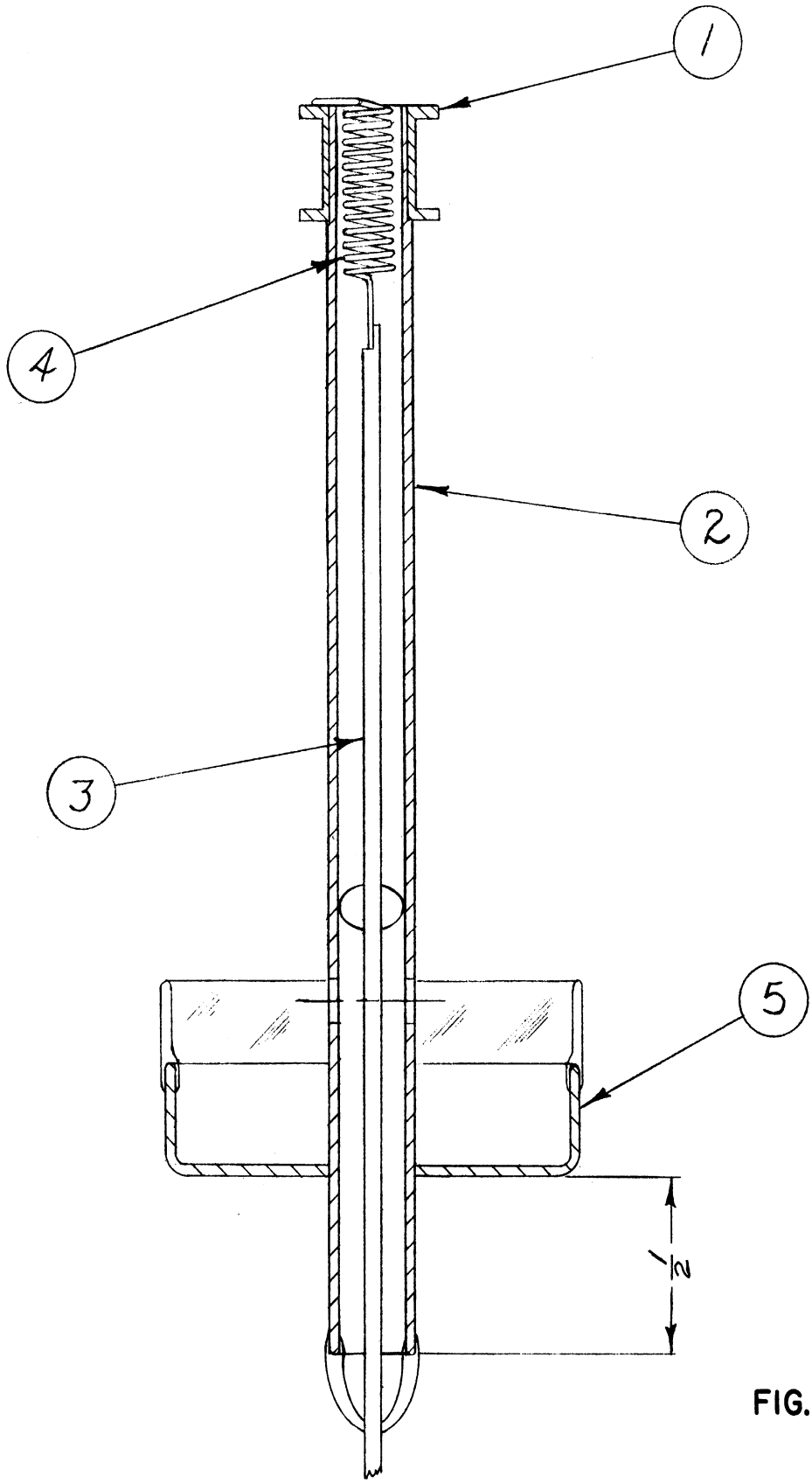

FIG. 5.6

ALL DIMENSIONS UNLESS OTHERWISE SPECIFIED MUST BE HELD TO A TOLERANCE - FRACTIONAL ± 1/64," DECIMAL ± .005," ANGULAR ± ½°

ISSUE	DATE

ENGINEERING RESEARCH INSTITUTE
UNIVERSITY OF MICHIGAN
ANN ARBOR MICHIGAN

PROJECT M-762

CLASSIFICATION

DESIGNED BY J K B	APPROVED BY
DRAWN BY M M	SCALE 2X
CHECKED BY J K B	DATE 12-7-46

TITLE OXIDE-COATED CATHODE

DWG. NO. A-8017

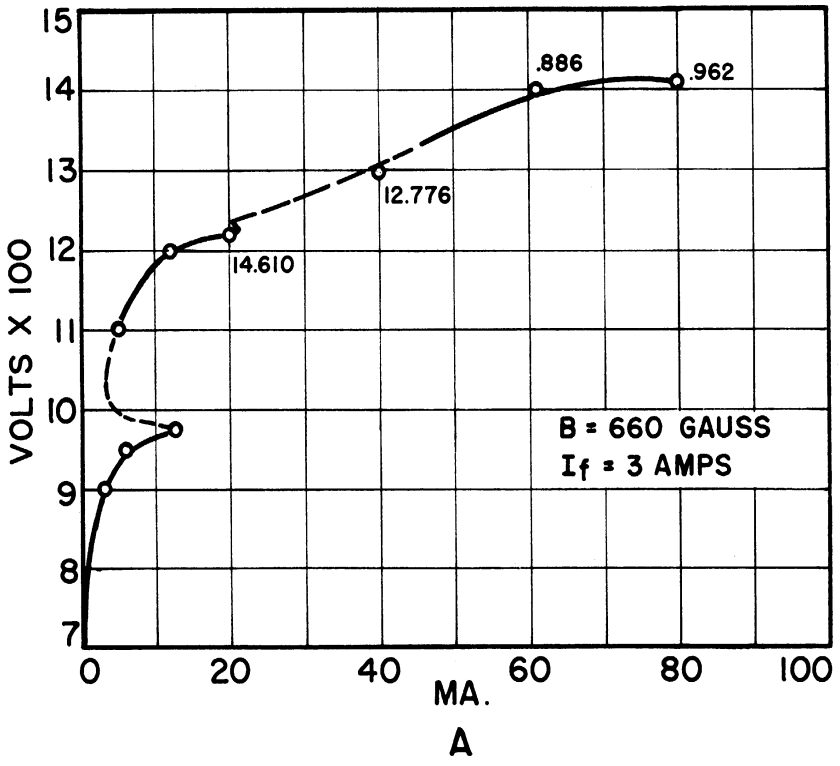

A

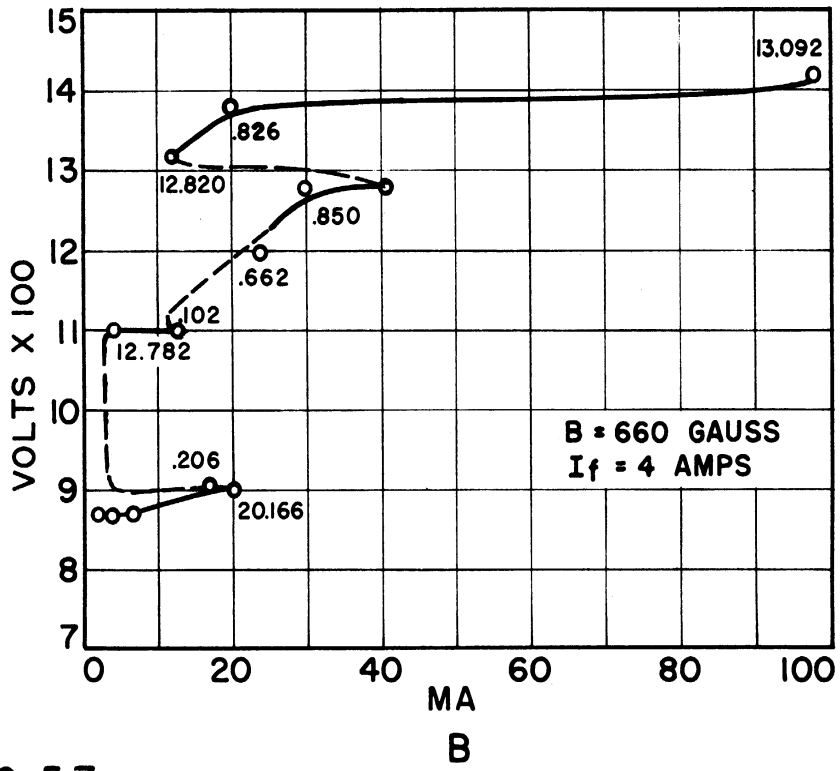

B

FIG. 5.7
VOLT AMPERE CHARACTERISTICS MODEL 7E 45

A small diameter filamentary cathode of carburized thoriated tungsten (manufactured by Litton Industries, Inc.) has been inserted into the Model 7A shell, minus any internal blocking filter in the cathode line. This particular model is distinguished by an extra output loop in the vane structure, with no backing ring. Fig. 5.8 is a drawing of this cathode structure. An external transmission-line arrangement is to be used on the cathode, allowing the input impedance to the cathode line to be varied. It will also be possible with this arrangement to measure the r-f power transmitted down the cathode line. Diode emission for the tube is about 2 amperes for the ratio of anode-to-cathode radii of 2.47. This tube has operated only in the vane mode when used without any cathode-line bypassing arrangement. A 14-cm mode exists but with insufficient power to give wavemeter readings. It was indicated by standing-wave minima positions in a slotted line.

Flux measurements have been made for the magnet geometry of Models 7A to 7E. These have hollow pole pieces; whereas, the 7F has one hollow pole piece and one solid pole piece. Fig. 5.9 is a flux map obtained experimentally. Fig. 5.10 gives the flux density vs. magnetic-field current. Curve 1 of this figure represents the values taken at the midpoint between the pole faces on the axis of symmetry; curve 2 gives the average value of B in the interaction space on a line bisecting the axis of symmetry at the midpoint; and curve 3 gives values for the field as measured by the flip coil method used in the past, for comparison to the present data obtained with a rotating-coil meter. Fig. 5.11 presents the field measurements as a function of distance from the axis of symmetry on a line passing halfway between the pole faces and on a line passing 1/8-in. from one pole face. Note the wide variation of field in the interaction space. On the center line, the field decreases with distance from the axis, whereas, it increases with distance on a line near

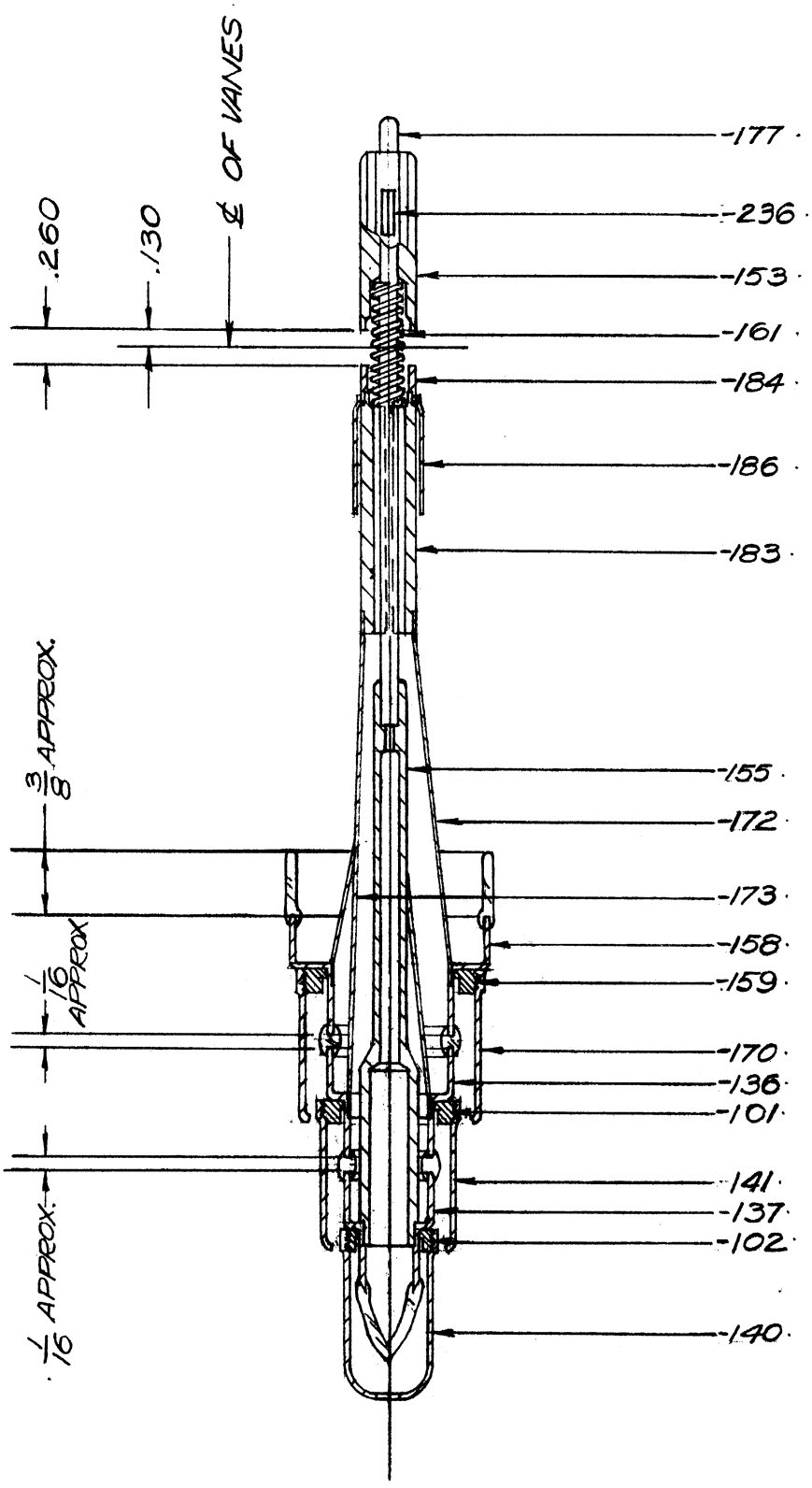

FIG. 5.8

NOTE: DESIGNED BY LITTON ENGINEERING LABORATORIES, REDWOOD CITY, CAL, "CATHODE ASSEMBLY — 6J21", DWG. L3000-203

ALL DIMENSIONS UNLESS OTHERWISE SPECIFIED MUST BE HELD TO A TOLERANCE - FRACTIONAL ± 1/64," DECIMAL ± .005," ANGULAR ± ½°

DEPARTMENT OF ENGINEERING RESEARCH UNIVERSITY OF MICHIGAN ANN ARBOR MICHIGAN		DESIGNED BY	APPROVED BY
		DRAWN BY JMW	SCALE FULL SIZE
		CHECKED BY R.S. Burwig	DATE 1/9/46
PROJECT M-694		TITLE CATHODE ASSEM.	
1 ISSUE	1/9/46 DATE	CLASSIFICATION	DWG. NO. A-8001

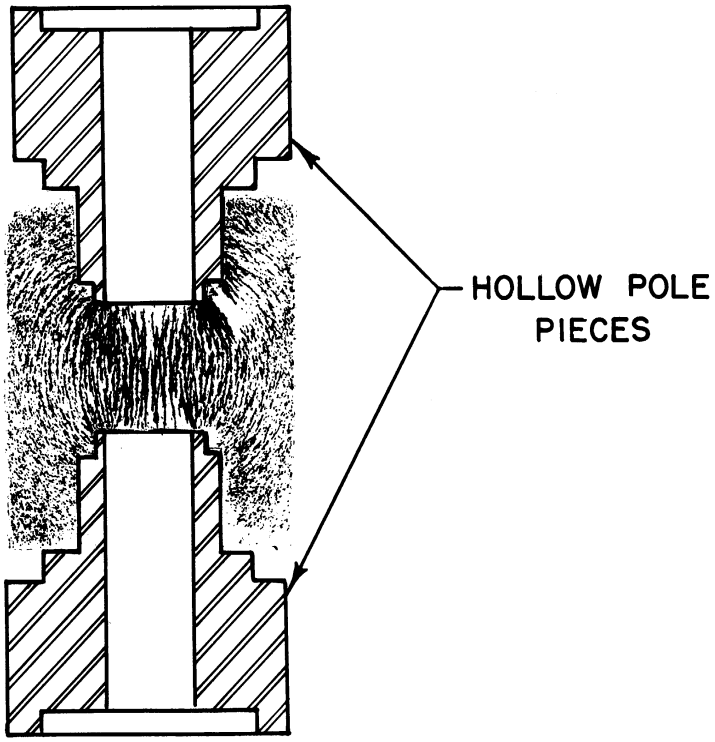

FIG. 5.9

MAGNETIC FIELD FLUX MAP FOR MODELS 7A-7E

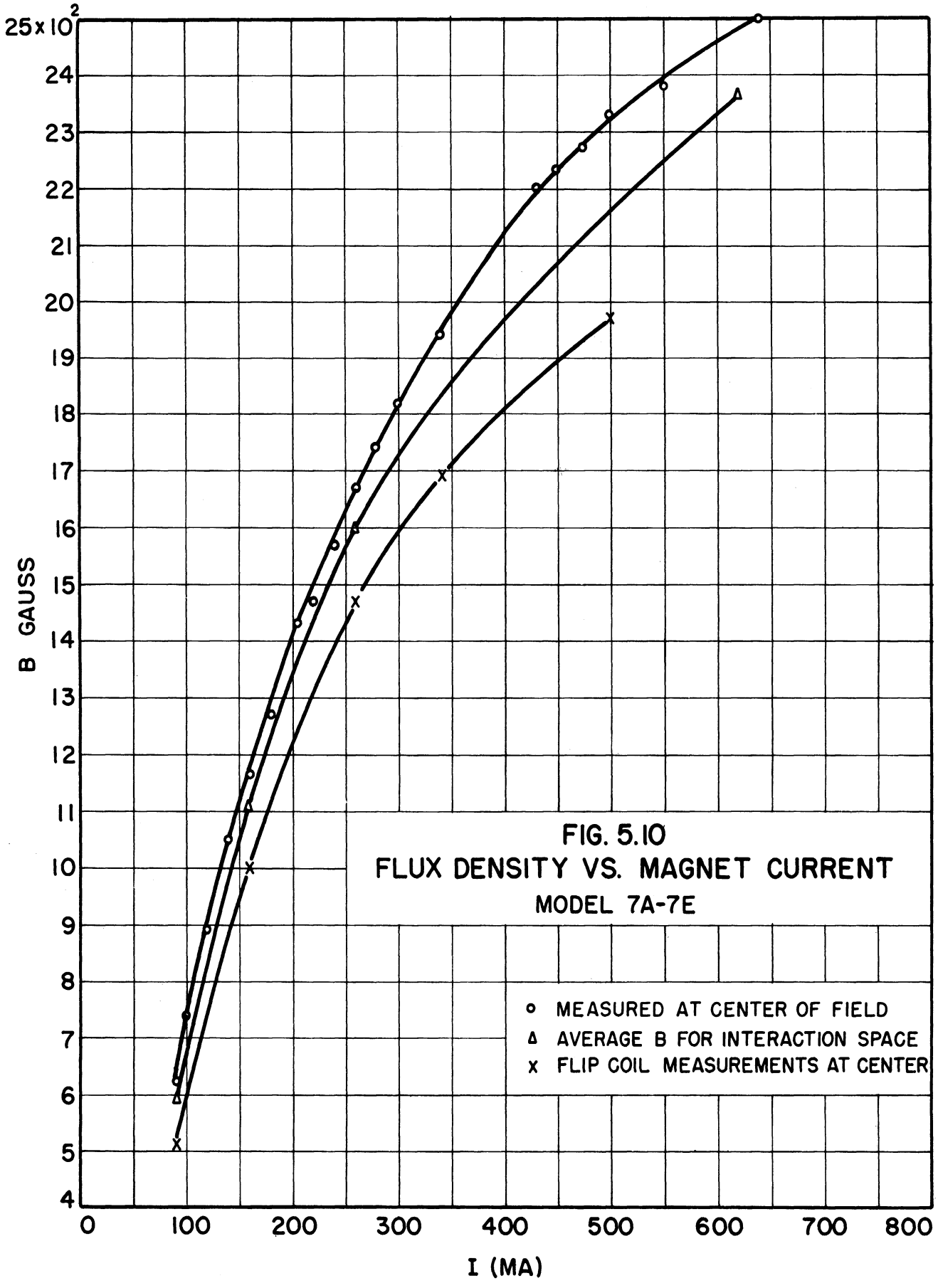
25x10²
24
23
22
21
20
19
18
17
16
15
14
13
12
11
10
9
8
7
6
5
4
B GAUSS
0
100
200
300
400
500
600
700
800
I (MA)
FIG. 5.10
FLUX DENSITY VS. MAGNET CURRENT
MODEL 7A-7E
o MEASURED AT CENTER OF FIELD
Δ AVERAGE B FOR INTERACTION SPACE
x FLIP COIL MEASUREMENTS AT CENTER

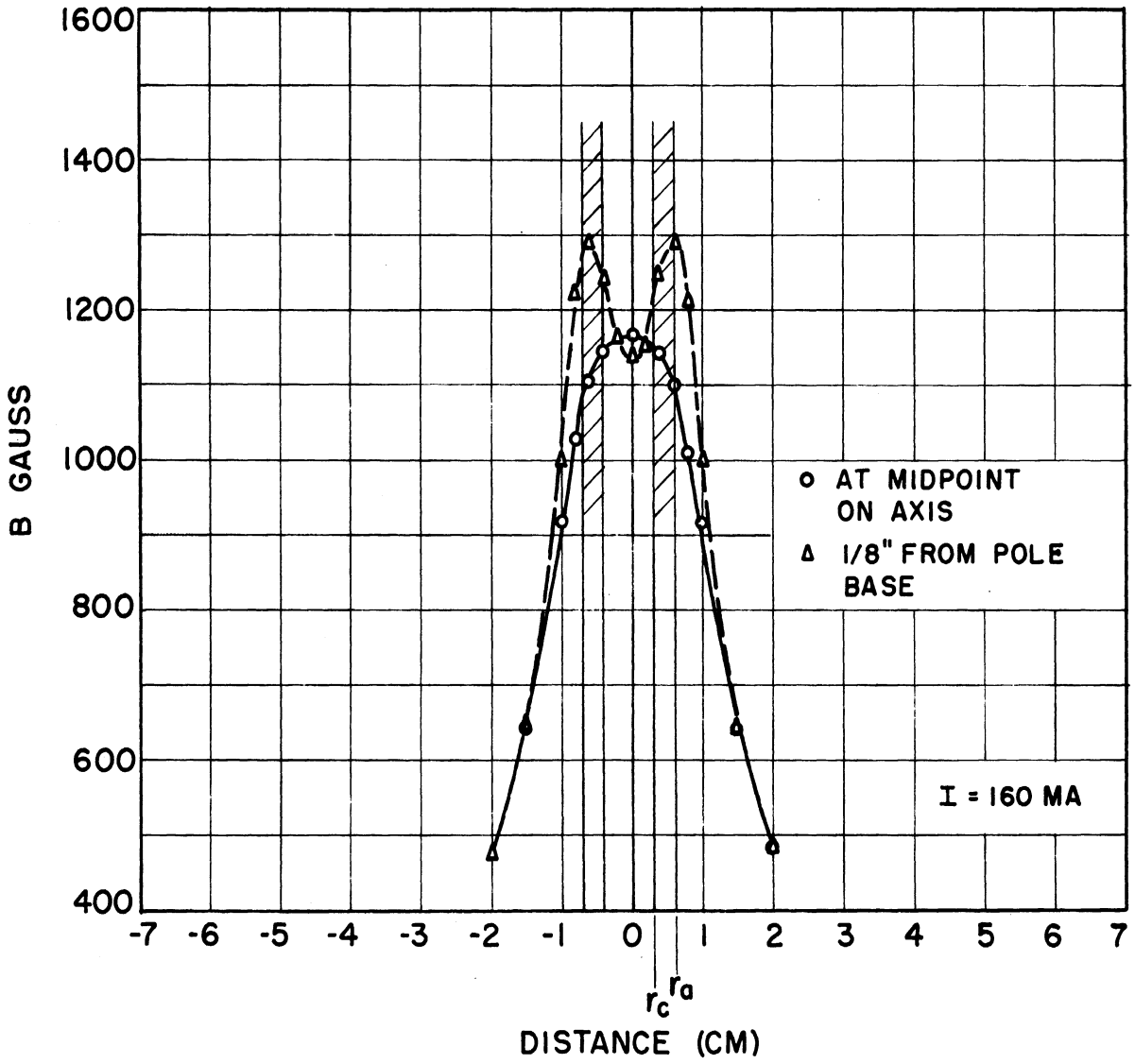

FIG. 5.11

FLUX DENSITY VS. DISTANCE FROM AXIS, MODEL 7A-7E

the pole faces. This is seen in the concentration of flux lines at the pole faces in Fig. 5.9.

6. The Trajectron — An Experimental D-C Magnetron (W. Peterson)

The main purpose of this experiment is to attain a more complete understanding of magnetrons by studying the space charge in a smooth-bore magnetron.

The tube which will be used for this work is a d-c smooth-bore magnetron with an electron gun in the same envelope arranged so that a beam of electrons can be sent into the space charge in an axial direction just grazing the cathode. The exit point of the beam will show on a fluorescent screen, thus an electron's position as a function of time after it leaves the cathode may be measured. From this information electron velocities at any radius may be calculated and the space-charge distribution determined.

The trajectron has been redesigned for use on a continuously-pumped system. The vacuum station is operating. The tube parts have been constructed and the tube is assembled and ready to be pumped down.

The diode section of the new trajectron has in it no magnetic materials. This should eliminate the difficulty experienced in the first model in aligning the electron beam. The continuous pumping system will also keep the tube from becoming gassy.

The seals at the ends of the diode anode are made with Teflon gaskets. The cathode assembly can be removed, and a spare cathode has been made. Thus the tube can be opened, the cathode and the fluorescent screen changed, and the tube sealed again in less than an hour. Changing an electron gun will take only a few hours. Thus this tube can be modified with relative ease.

The cathode of the new tube has a bifilar heater to minimize the magnetic field from this source.

A convenient high-voltage low-current supply has been constructed to be used with the electron gun. It is of the type used in television receivers, and voltage regulation is incorporated in it.

7. Theoretical Analysis of Frequency Pushing and Voltage Tuning (H. W. Welch, Jr.)

Substantial progress has been made during the last quarter toward obtaining a theoretical understanding of frequency pushing and voltage tuning. This theory will be presented in detail with experimental confirmation in a forthcoming technical report. The following brief treatment will summarize some of the essential points of the analysis and indicate its applicability to practical problems.

In order to predict completely oscillatory magnetron performance in terms of the picture of the space charge which has been used in previous Michigan reports and other references,[1] the following facts must be known: geometry of the space-charge swarm including boundaries of the spoke configuration, the density distribution of electrons in the spokes, the interaction-space geometry, the impedance between anode sets as a function of frequency, and the average velocity of the spokes around the cathode, as well as the drift velocities of electrons through the spokes. The space-charge-swarm behavior depends, not only on the d-c voltage and magnetic field, but on the r-f voltage between anode sets. The problem is thus a self-consistent one since the r-f voltage depends on the current induced by the spokes and the spoke geometry depends on the r-f voltage. This is in addition to the

---

[1] See Technical Report No. 5.

self-consistency required to take account of the Poisson field of the space charge.

In Technical Report No. 5, we have attempted to develop an approximately quantitative method for the calculation of the induced current which will result from a spoke configuration resulting from a given anode voltage. The method summarized here serves to predict by a relatively simple analysis the approximate spoke geometry and phase relationship of the spoke of charge to the r-f voltage wave on the anodes for various specified conditions. If the phase relationship is known, the required phase of the load is predictable. If the magnitude of the current is known for a given r-f voltage, the required magnitude of the load impedance is predictable. The method is not complete but very definite conclusions can be proposed relative to the frequency-pushing and voltage-tuning phenomena.

If one considers the electron in the reference frame moving with the velocity synchronous with the r-f wave in the magnetron interaction space, effects of time variation of the electromagnetic fields are approximately erased. This is based on the assumption that the electron interacts only with the wave which moves around the interaction space in the same direction as the drift motion of the electron. Under these conditions it can be shown that, in order for an electron to reach a point a given distance from the cathode surface, a certain threshold energy must have been delivered to the electron. If it is assumed that the electron acquires all of its energy from the electric field, then the electrical potential of the point must exceed this threshold energy in electron volts. The threshold anode potential is the Hartree potential, given in the cylindrical magnetron by

$$\phi_{aT} = \frac{1}{2} B \left(\frac{2\pi f}{n}\right)(r_a^2 - r_c^2) - \frac{1}{2}\left(\frac{2\pi f}{n}\right)^2 \frac{m}{e} r_a^2 , \qquad (7.1)$$

where

$\frac{2\pi f}{n}$ = $\frac{2\pi \text{ x oscillatory frequency}}{1/2 \text{ number of anodes}}$ = synchronous angular velocity

r_a = anode radius

r_c = cathode radius

ϕ_{aT} = threshold potential

It is proposed, as was proposed by Hartree, that, in order for electrons to reach the anode, this threshold potential must be exceeded on the anode. If rf exists on the anode this condition may be satisfied over only part of the cycle, as is illustrated in Fig. 7.1a. The threshold potential is represented by the line labeled ϕ_{aT}, the actual d-c anode potential by ϕ_a, and the peak value of the fundamental travelling-wave component of the r-f voltage between anode segments by ϕ_f. The spoke of the electrons must end on the anode between the points A and B, represented by the shaded area. Thus the position of the spoke is approximately located. However, if the spoke is symmetrically distributed about the positive voltage maximum, analysis will show that the current induced into the circuit must be exactly 90°, lagging the r-f voltage so that the circuit must be a pure inductive reactance at the frequency of the induced current. No power is transferred from the electrons to the r-f field.

Another restrictive condition is illustrated by Fig. 7.1b. It can be shown that, in a region between the positive and negative r-f potential maxima, C and E, electrons will have a component of drift motion toward the anode. In the region between D and C, there will be a component of drift motion away from the anode. Since all of the electrons originate at the cathode, it will be expected that the spoke will end on the anode between C and B.

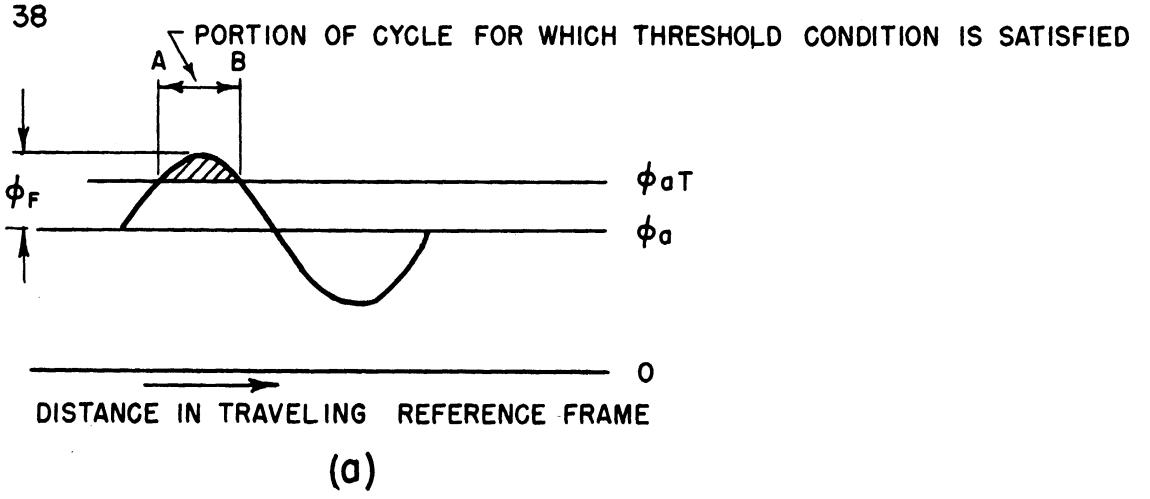

(a)

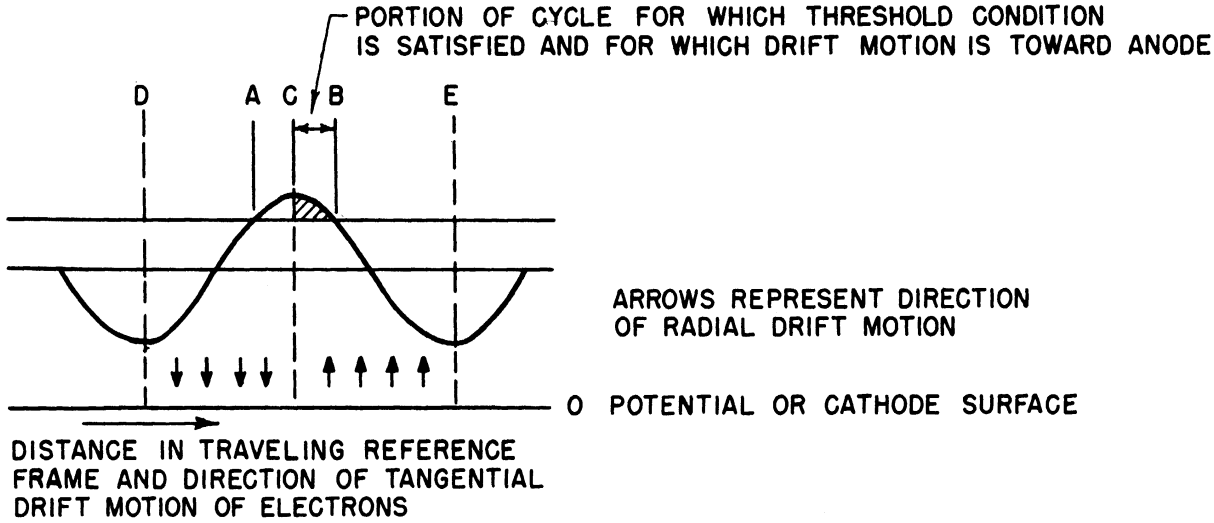

(b)

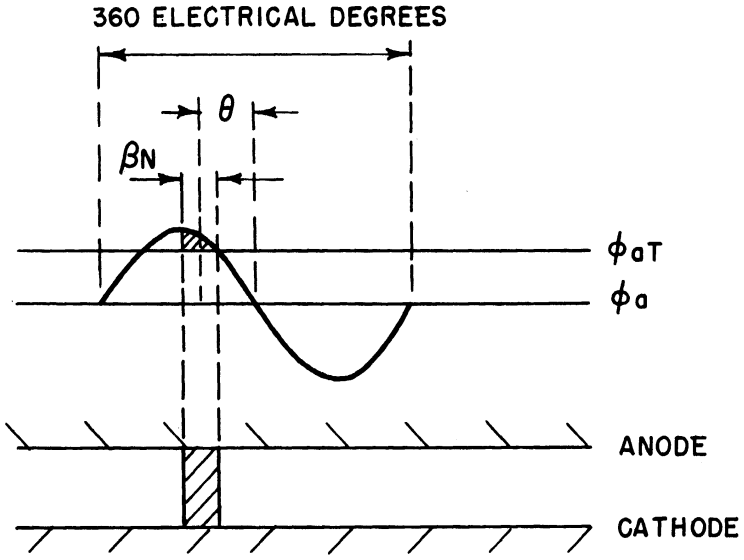

(c)

FIG. 7.1
ILLUSTRATION OF GRAPHICAL METHOD FOR DETERMINING SPOKE WIDTH AND PHASE ANGLE

The region between A and C is ruled out because the drift motion is away from the anode where no electrons originate.

In Fig. 7.1c, the end result of such a diagram is shown. The approximate position of the spoke is represented as a shaded area between an anode and cathode surface in its proper relationship to the r-f voltage wave (fundamental travelling component). A full cycle of the r-f wave is 360 electrical degrees. Actually, in space, a full cycle occupies only $720°/N$, where N is the number of anode segments. The phase angle between the induced current and the r-f voltage between segments can be shown to be given by θ. The width of the spoke is βN electrical degrees, where β is the actual space width in degrees (notation used in Technical Report No. 5, page 85). θ, in Fig. 7.1c, is less than 90°; electrons are drifting toward the anode so d-c power is supplied to the system and r-f power is supplied to the circuit. These are the conditions for oscillation.

Certain facts can be pointed out and the method qualitatively illustrated with reference to Fig. 7.2.

For a given space-charge density it can be shown that the maximum induced current will be obtained for $\beta N = 180°$. Thus, in Figs. 7.2a, b, and c, the induced current would be progressively increasing. In order for this to happen and the r-f voltage to remain constant, as is assumed, the circuit impedance would have to be decreased, as is indicated in the captions. It is also necessary to raise the anode voltage to produce larger values of βN. This means that one would expect the anode voltage, for a given r-f voltage amplitude and frequency, to increase with a decrease in Q. This is the experimentally observed fact. The small change in frequency associated with the change in circuit phase angle θ will result in a small change in ϕ_{aT}

(a) HIGH IMPEDANCE CIRCUIT (HIGH Q)

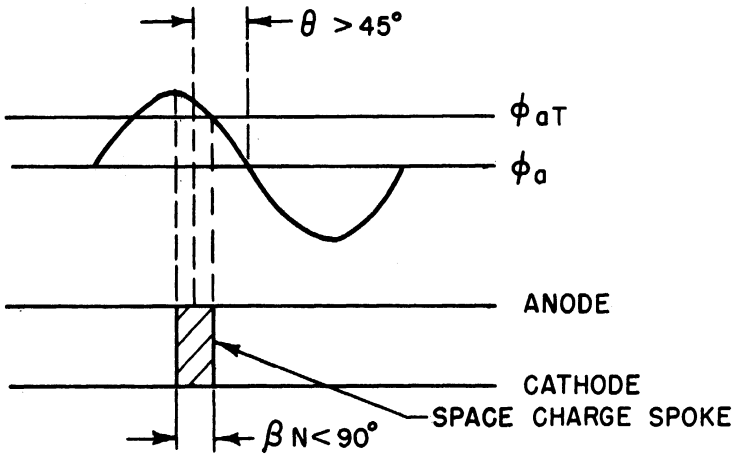

ANODE VOLTAGE FIRST REACHES ϕ_{aT} THEN JUMPS DOWN TO ϕ_a AT FINITE CURRENT AND POWER

(b) MEDIUM IMPEDANCE CIRCUIT (MEDIUM Q)

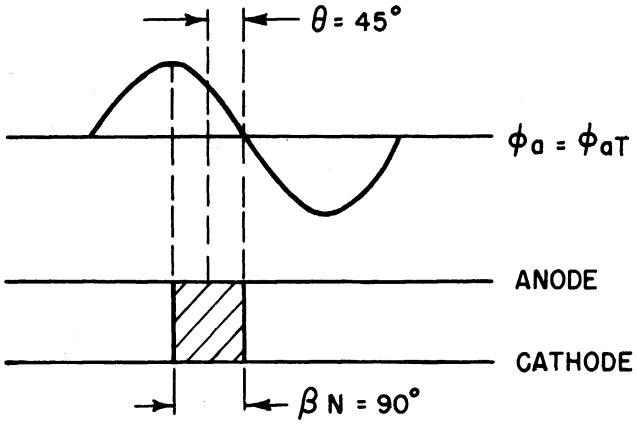

(c) LOW IMPEDANCE CIRCUIT (LOW Q)

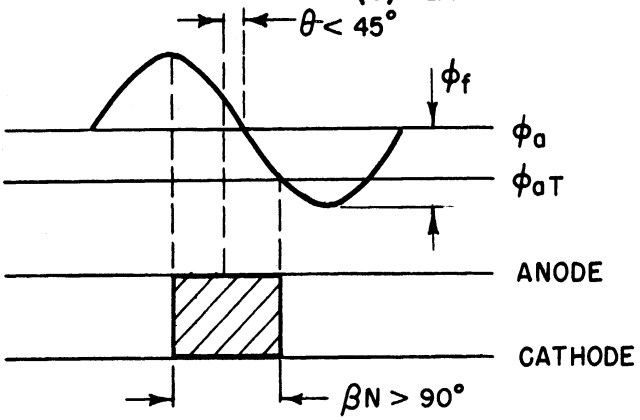

FIG. 7.2

ILLUSTRATION OF EFFECT OF VARIOUS CIRCUIT CONDITIONS ON SPACE-CHARGE BEHAVIOR. R-F VOLTAGE AND SPACE-CHARGE DENSITY ASSUMED CONSTANT.

(from Eq 7.1). However, for a circuit with reasonably high Q's, this change is negligible.

The pictures of Fig. 7.2 could also be used to represent normal operation into a resonant circuit if the r-f voltage amplitude were made progressively greater from a to b to c. This would happen for two reasons: the induced current is growing larger and the circuit impedance is increasing with decreasing positive phase angle. An important critical condition is expected when the phase angle becomes zero. For this condition

$$\phi_a - \phi_{aT} = \phi_f \,, \tag{7.2}$$

$$\beta N = 180^\circ \,,$$

$$\theta = 0 \,,$$

where ϕ_f = peak value of fundamental travelling r-f wave.

The induced current is now a maximum for a given charge density; for higher d-c voltages, the threshold voltage is always exceeded, the spoke tries to become broader than 180° but is discouraged from doing so by the direction of the drift motion; also, for higher voltages the frequency tends to go up, forcing the spokes to induce current into a capacitive circuit, the r-f voltage tends to decrease and the focussing forces forming the bunches are reduced. In short, the tube would be expected to cease operating.

The discussion just given applies to a resonant circuit where the phase angle is a rapidly varying function of frequency so that ϕ_{aT} does not vary appreciably as ϕ_a is increased. The decrease in phase angle with increasing ϕ_a represents an increased delivery of r-f power to the circuit. The increasing "conduction angle" βN represents an increase in d-c current and, therefore, power input.

Let us suppose another condition, namely, a high-impedance inductive non-resonant circuit. This is represented by Fig. 7.2a. Furthermore, let us suppose that temperature-limited conditions prevail at the cathode so that the d-c current through the spoke is limited. Presumably, then, the conditions shown in Fig. 7.2a satisfy the self-consistent relationship between r-f voltage, circuit impedance, and spoke configuration for the available d-c current. Now suppose that the anode voltage is raised. The spoke will tend to speed up, thus increasing the synchronous-wave velocity, but the phase will not change rapidly with frequency. Moreover, if ϕ_a tends to increase relative to ϕ_{aT}, βN would become larger, tending to require more d-c current. This current is not available since we have specified temperature-limited conditions. The expected result is therefore that ϕ_a and ϕ_{aT} will both be raised when ϕ_a is increased and the frequency will increase as demanded by Eq 7.1. The whole pattern will rise relative to the zero of potential. These are the required conditions for voltage tuning.

The critical condition mentioned above for $\phi_a - \phi_{aT} = \phi_f$ is important in the consideration of the proper circuit for voltage-tuning operation. It was indicated in the discussion of this condition that operation into a capacitive circuit would be unsatisfactory or impossible. Thus to achieve voltage tuning, one should use a very low-Q circuit on the inductive side of resonance, or a non-resonant inductive circuit, or a completely non-reactive high-impedance circuit.

The conclusions briefly summarized here seem to be borne out by preliminary examination of experimental data obtained in this laboratory and elsewhere. More complete substantiation of these remarks with experimental confirmation, will be given in a forthcoming technical report. The following

conclusions may be offered on the basis of the preceding discussion and experimental evidence which has been examined by the author.

In normal operation, the maximum frequency pushing to be expected will be given by the frequency change associated with a circuit phase angle change of between 60° to 80° and 0°. This is a little greater than 1/2 Q_L x f_o where f_o is the oscillatory frequency and Q_L is the loaded Q.

Observed frequency pushing may be less than the maximum figure if the phase angle change for some reason covers only part of the maximum expected range (i.e., 75° to 45°) over the useful volt-ampere characteristic.

The frequency pushing per ampere may be made smaller if the slope of the volt-ampere characteristic can be increased. This has been definitely observed in one case where the slope was increased by causing the cathode to operate temperature-limited. Other methods probably can be used and this possibility will be considered in the future.

Voltage tuning with a temperature-limited cathode will be limited to the frequency range for which the circuit has a phase angle ≥ 0. For example, a circuit which is a pure resistance of the required impedance magnitude for all frequencies should permit very wide voltage tuning at constant power. An inductive circuit would not be expected to give constant power. This conclusion is based on the premise that the space-charge-spoke behavior is independent of frequency. It is actually a slowly varying function of frequency and this would have to be considered in an exact analysis.

8. Propagation of Electromagnetic Waves in the Plane Magnetron Space Charge in the Direction of the Steady Electron Motion (G. R. Brewer)

The propagation of electromagnetic waves in the direction parallel to the steady electron velocity in the magnetron should prove of interest from

two points of view. While this analysis is carried out only for the plane magnetron the general results should be applicable, at least qualitatively, to considerations involving the cylindrical magnetron, and might be of assistance in explaining certain frequency effects of the space charge on the resonant circuit, such as frequency pushing and voltage tuning. Secondly, it is believed (as has been suggested by a number of people) that a magnetron structure should be capable of providing amplification of electromagnetic waves. This possibility was suggested earlier in the course of this work,[1] the idea being based partly on an analysis carried out at that time and partly on intuitive considerations, extrapolating from the successful Electron Wave Tube[2] due to Haeff. The analysis presented in the aforementioned report (reference 1 on this page) has since been found to be incorrect; however, the possibility of amplification has not been abandoned.

The problem of wave propagation in the direction of electron motion in a plane magnetron space charge has been treated in a comprehensive manner by Macfarlane and Hay.[3] However, while they apparently found suitable mathematical expansions enabling rather general solution of the equations, some of their most interesting results are not presented for the case of the magnetron (their case $\alpha = 1$). That is, they consider interaction with a

---

1 Quarterly Progress Report No. 2, Electron Tube Laboratory, University of Michigan, July, 1950.

2 Haeff, A. V., "The Electron Wave Tube — A Novel Method of Generation and Amplification of Microwave Energy", Proc. I.R.E., 37, pp 4-10, 1949.

Labus, J., "High Frequency Amplification by Means of the Interaction Effect between Electron Streams", Arch. Elekt. Ubertragung, 4, pp 353-360, 1950.

3 Macfarlane, G. G., and Hay, H. G., "Wave Propagation in a Slipping Stream of Electrons: Small Amplitude Theory", Proc. Phys. Soc., Lond., B, LXIII, pp 409-427, 1950.

beam of electrons injected between two parallel structures, the electron velocity varying linearly with distance normal to these structures, but not vanishing at one of them as in the magnetron with a cathode as one element of the delay line.

This problem of amplification in a plane magnetron structure has also been mentioned in a note by Buneman.[1]

Therefore, while the present treatment of this problem will necessarily be of more limited scope than that of Macfarlane and Hay, it is hoped that the results can be applied profitably to the magnetron.

For consideration of electromagnetic wave propagation in the direction parallel to the steady or drift velocity of the electrons, two types of waves must be distinguished. The first wave will propagate with a velocity near that of light, being determined by the dielectric properties of the space charge as well as the boundary conditions imposed by the confining circuit. A possible example of this case would be wave propagation along a plane parallel transmission line, one of whose elements is an emitter, giving rise to a space charge with drift velocity along the length of the line. Since this case is of little practical interest, it will not be treated here.

The second type of wave involves propagation along a structure (usually periodic in space) such that the phase velocity of the wave is considerably less than the velocity of light. This structure is usually made as some type of periodically loaded transmission line, such as a loaded wave guide (the side opposite the "slow wave" structure being an emitter) and the wave velocity can be made (within reason) to conform to the designer's wishes, usually one-tenth or less the velocity of light. This low value of wave

---

[1] Buneman, O., "Generation and Amplification of Waves in Dense Charged Beams under Crossed Fields", Nature, 165, p. 474, March, 1950.

velocity allows certain simplifications to be made in the equations, as will be seen later.

The essential differences between the "field wave" and the "space-charge wave" can then be summarized as follows. In the field wave, which is propagated with a phase velocity near to that of light, the space-charge density exerts relatively little influence on the fields; that is, there is relatively little wave energy stored in the electron motions, so that this wave is characterized by $\nabla \cdot E \cong 0$ (the wave energy in this case being stored alternately in the electric and magnetic fields). The space-charge wave, propagating with a phase velocity small compared with that of light, is influenced to a great extent by the space charge; in fact the wave energy is stored alternately in the electric field of the wave and in the kinetic energy of the electrons. Since in this case there is relatively little energy stored in the magnetic fields, this wave type can be characterized by $\nabla \times E \cong 0$.

Propagation along a "Slow Wave" Structure. A schematic drawing of the structure to be used for illustrative purposes in the following analysis is shown in Fig. 8.1. It is assumed that the electron velocity is slow compared to the velocity of light so that the treatment is non-relativistic and also the usual small signal method is used. In addition, it is assumed that the wave velocity is small compared to the velocity of light so that the time rate of change of magnetic field can be neglected, and the electric field derived from a potential function. Then $\nabla \times E \cong 0$[1] and the field components present are E_x, E_y, and H_z.

---

[1] The degree of approximation of this customary simplification can be seen by writing the electric field in terms of the vector potential A and the scalar potential ϕ as:

$$E = -\nabla \phi - \frac{\partial A}{\partial t}$$

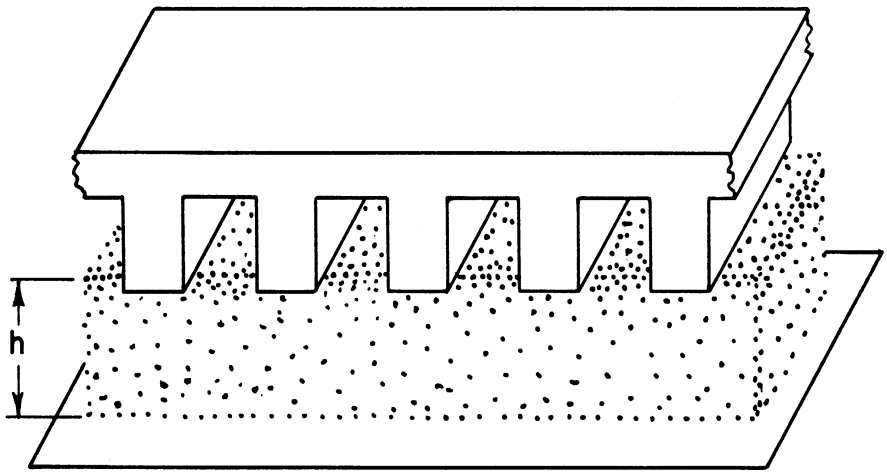

FIG. 8.1
IDEALIZED SPACE CHARGE IN PLANE MAGNETRON WITH PERIODIC ANODE

Fig. 8.1

(Cont'd. from page 46) and using the supplementary condition on A:

$$\nabla \cdot A = - \mu \epsilon \frac{\partial^2 \phi}{\partial t^2} .$$

Then:

$$\nabla \cdot E = - \nabla^2 \phi + \frac{1}{c^2} \frac{\partial^2 \phi}{\partial t^2} .$$

Considering the potential to represent a wave motion in the x direction so that $\phi = \phi_0 e^{i\omega t - \gamma x}$

$$\nabla \cdot E = - \gamma^2 \phi + \frac{\omega^2}{c^2} \phi ,$$

so that when $\omega^2/c^2 \ll \gamma^2$ this last term can be neglected and $E = - \nabla \phi$.

The equations of motion are, assuming the perturbation velocities to vary as $e^{i\omega t - \gamma x}$:

$$\begin{aligned} i\omega\, v_x - \gamma v_o\, v_x &= -\frac{e}{m} E_x , \\ i\omega\, v_x - \gamma v_o\, v_y &= -\frac{e}{m} E_y - \omega_c v_x , \end{aligned} \tag{8-1}$$

and from these, the electron velocities are:

$$v_x = \frac{-\frac{e}{m} E_x}{i\omega + \gamma \omega_c y}, \qquad v_y = \frac{-\frac{e}{m} E_y}{i\omega + \gamma\omega_c y} - \frac{\frac{e}{m}\omega_c E_x}{(i\omega + \gamma\omega_c y)^2} , \tag{8-2}$$

where the substitution $v_o = -\omega_c y$ has been made. In this, it is implicitly assumed that the cathode is located at $y = 0$. The field equations are:

$$\begin{aligned} -\gamma E_y &= \frac{\partial E_x}{\partial y} , \qquad \frac{\partial H_z}{\partial y} = \rho_o v_x + v_o \rho_1 + i\omega \epsilon_o E_x , \\ \rho_1 &= \epsilon_o\left(-\gamma E_x + \frac{\partial E_y}{\partial y}\right), \quad \gamma H_z = \rho_o v_y + i\omega \epsilon_o E_y . \end{aligned} \tag{8-3}$$

Performing the indicated differentiations and combining these expressions, Eqs 8-2 and 8-3, the following differential equation is obtained.

$$\begin{aligned} &\left[A + (i\omega + \gamma\omega_c y)\,\epsilon_o\right]\frac{1}{\gamma}\frac{\partial^2 E_x}{\partial y^2} + \left(\frac{1}{\gamma}\frac{\partial A}{\partial y} + C\right)\frac{\partial E_x}{\partial y} \\ &\quad + \left[\frac{1}{\gamma}\frac{\partial C}{\partial y} + A + (i\omega + \gamma\,\omega_c y)\,\epsilon_o\right]\gamma E_x = 0 , \end{aligned} \tag{8-4}$$

where

$$A = \frac{-\rho_o\, e/m}{i\omega + \gamma\omega_c y}$$

$$C = \frac{\rho_o\, e/m\, \omega_c}{(i\omega + \gamma\omega_c y)^2} .$$

This equation will be simplified by substitution of the new variable:

$$\ell = \frac{\omega}{\omega_c}\left(1 + \frac{\gamma \omega_c y}{i\omega}\right). \tag{8-5}$$

Then Eq 8-4 becomes:

$$\left(\ell - \frac{1}{\ell}\right)\frac{\partial^2 E_x}{\partial \ell^2} + \frac{2}{\ell^2}\frac{\partial E_x}{\partial \ell} - \left(\frac{2}{\ell^3} - \frac{1}{\ell} + \ell\right) E_x = 0 . \tag{8-6}$$

This is the basic differential equation representing the electric field in the space-charge region and presupposes only that the velocity of the wave in the space charge is small compared with the velocity of light. In what follows, the exact nature of the external circuit will not be specified, it being presumed that a circuit of the characteristics desired to achieve certain performance can be constructed. It is seen from Eq 8-5 that Re $\ell = 0$ corresponds to synchronism between a layer of electrons at distance y above the cathode and a wave travelling in the -x direction.

Since the most interesting interaction effects take place for velocities near this synchronism condition, in what follows the attention will be confined to small values of ℓ. Therefore, the solution to Eq 8-6 will be found in terms of a power series expansion in ℓ.

Therefore, let:

$$E_x = \sum_0^\infty a_n \ell^n , \tag{8-7}$$

from which it follows:

$$\frac{\partial E_x}{\partial \ell} = \sum_0^\infty n\, a_n \ell^{n-1} ,$$

$$\frac{\partial^2 E_x}{\partial \ell^2} = \sum_0^\infty n(n-1)\, a_n \ell^{n-2} .$$

Substituting these into Eq 8-6, the following recursion relation is found:

$$- \sum_{0}^{\infty} \left[n(n-3) + \right] 2\, a_n \ell^{n-3} + \sum_{0}^{\infty} \left[n(n-1) + 1 \right] a_n \ell^{n-1} - \sum_{0}^{\infty} a_n \ell^{n+1} = 0 \ ,$$

so that the first few coefficients are:

$a_0 = 0$		$a_1 =$ arbitrary		$a_{10} = .1475\, a_2$	
$a_2 =$ arbitrary		$a_3 = a_1/2$		$a_{11} = .0760\, a_1$	
$a_4 = a_2/2$		$a_5 = 5/24\, a_1$			
$a_6 = 11/40\, a_2$		$a_7 = 93/720\, a_1$			
$a_8 = 321/1680\, a_2$		$a_9 = 3848/40320\, a_1$			

The boundary condition to be imposed on the electric field E_x in the space charge is that it must vanish at the cathode, i.e., $E_x = 0$ when $y = 0$ ($\ell = \omega/\omega_c$). Under this condition, the solution of Eq 8-6 becomes:

$$\frac{E_x}{a_2} = - \frac{\omega}{\omega_c} \ell \left[1 + \frac{1}{2} \ell^2 + 0.21\, \ell^4 + 0.129\, \ell^6 + 0.0966\, \ell^8 + \ldots \right] + \ell^2 \left[1 + \frac{1}{2} \ell^2 + 0.275\, \ell^4 + 0.191\, \ell^6 + \ldots \right] . \tag{8-8}$$

It is seen that two independent series are obtained, one including the even and the other the odd powers of the variable quantity.

The electric field E_x in the space charge is shown in Fig. 8.2 plotted vs. Re ℓ from Eq 8-8 using the above specified boundary condition. Certain qualitative information concerning the space charge can be obtained from a study of these curves.

The cathode of the magnetron is, of course, represented by the right hand intersection with the abscissa of the curve corresponding to the particular value of ω/ω_c under consideration. The intersection at $\ell = 0$ corresponds

to synchronism between the layer of electrons at a given value of y and the travelling electromagnetic wave. It is seen that this synchronous layer of electrons becomes an infinite admittance sheet in the space charge. The portion of the curves to the right of $\ell = 0$ represent the field in the region in which the electrons are moving slower than the wave and the part to the left of $\ell = 0$ the region in which the electrons are moving faster than the wave. From this it appears that the interaction space in a magnetron is divided into two regions by this admittance sheet; the region between cathode and the infinite admittance sheet and the region between this sheet and the anode. As the electrons are caused to increase in velocity (e.g., by increasing the magnetic field), this sheet will be displaced toward the cathode.

Examination of Eq 8-4 reveals that in addition to the regular singular point at $\ell = 0$, this equation contains a second regular singular point at $\ell = \pm 1$. It will prove interesting to examine briefly the physical nature of this singularity also. For the value $\ell = -1$, the real part of Eq 8-5 becomes:

$$\omega_c = \omega\left(\frac{v_o}{v_p} - 1\right),$$

where v_p is the phase velocity of the wave propagating with the electron stream, i.e., $v_p = -\omega/\mathrm{Im}\,\gamma$. The right side of this relation is seen to be the frequency of the wave whose forces are acting on the electrons, as seen by the moving electrons. That is, while a stationary observer (an electron) experiences a force due to the fields of frequency ω, an observer moving with velocity v_o experiences a force of frequency $\omega(v_o/v_p - 1)$. Therefore, at the value of v_o/v_p for which this Doppler frequency is equal to the cyclotron frequency, the layer of electrons for which $\mathrm{Re}\,\ell = -1$ experiences a resonance effect between the wave and the applied magnetic field. From this, it would

be expected that the electric fields of the wave have a singularity[1] at the value Re ℓ = - 1. That this is indeed the case can be seen from Figs. 8.2 and 8.3.

The singularity at the point ℓ = + 1 is of less interest since this interaction (for $\omega/\omega_c < 1$) takes place below the cathode. However, this singularity corresponds to the same type of phenomenon, with electrons moving in the +x direction interacting with fields of Doppler frequency $\omega(1 - \frac{v_o}{v_p})$ of a wave travelling in the +x direction.

The admittance looking into the space-charge cloud can be determined by a method originally suggested by Hahn[2] in which the surface is assumed perturbed periodically in space by the propagating wave. The effect of these perturbations in the surface is considered to be represented by a surface current flowing in the plane of the unperturbed surface. The tangential magnetic-field component on the outside of the space charge can then be equated to the sum of the tangential magnetic field inside plus the surface current. This method of evaluation yields the following equation for the normal admittance:

$$Y_e = \frac{H_z(h)}{E_x(h)} = \left\{ \left(\frac{i\omega+2\gamma\omega_c h}{\gamma(\gamma\omega_c h+i\omega)} \right) \frac{-\rho_o\, e/m}{i\omega+\gamma\omega_c h} + \frac{i\omega\epsilon_o}{\gamma} \right\} \frac{E_y(h)}{E_x(h)} - \left(\frac{i\omega+2\gamma\omega_c h}{\gamma(\gamma\omega_c h+i\omega)} \right) \frac{\rho_o\, e/m\, \omega_c}{(i\omega+\gamma\omega_c h)^2} \quad (8\text{-}9)$$

where only wave propagation in the -x direction is considered.

---

1 It can be shown (A Course of Modern Analysis -- Whittaker and Watson, Cambridge, 1946, p. 201), that in such a case as considered here, the function will be either analytic or have a logarithmic singularity at the regular singular point. In view of the above mentioned account of the nature of the interaction at the singularity, the latter possibility appears more probable.

2 W. C. Hahn, "Small Signal Theory of Velocity-Modulated Electron Beam", G. E. Rev., 42, No. 6, June 1939, p. 258.

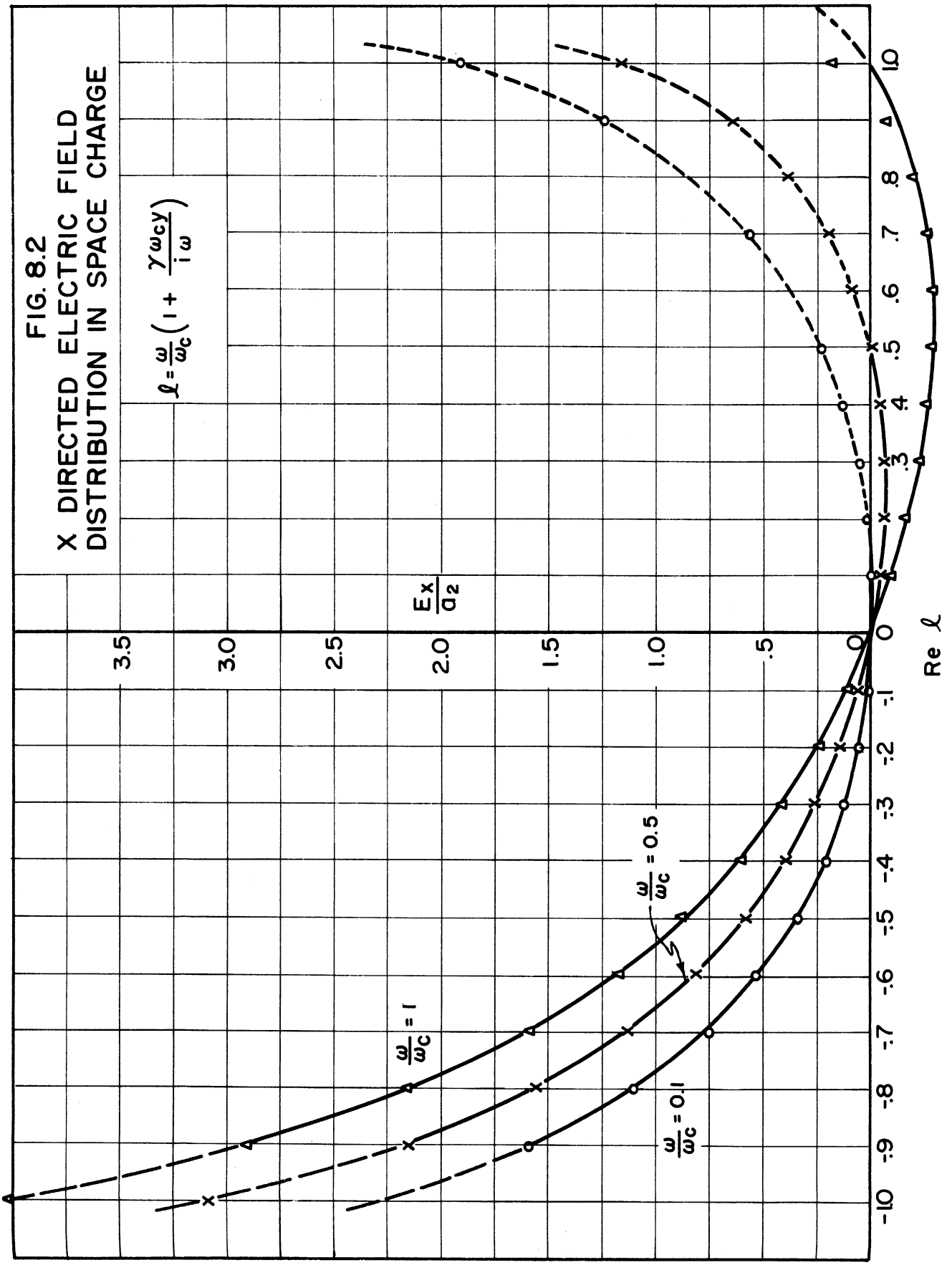
FIG. 8.2
X DIRECTED ELECTRIC FIELD
DISTRIBUTION IN SPACE CHARGE
$\ell = \frac{\omega}{\omega_c}\left(1 + \frac{\gamma\omega_{cy}}{i\omega}\right)$
$\frac{E_x}{\sigma_2}$
3.5
3.0
2.5
2.0
1.5
1.0
.5
0
$\frac{\omega}{\omega_c} = 1$
$\frac{\omega}{\omega_c} = 0.5$
$\frac{\omega}{\omega_c} = 0.1$
-10 -9 -8 -7 -6 -5 -4 -3 -2 -1 0 .3 .4 .5 .6 .7 .8 1.0
Re ℓ

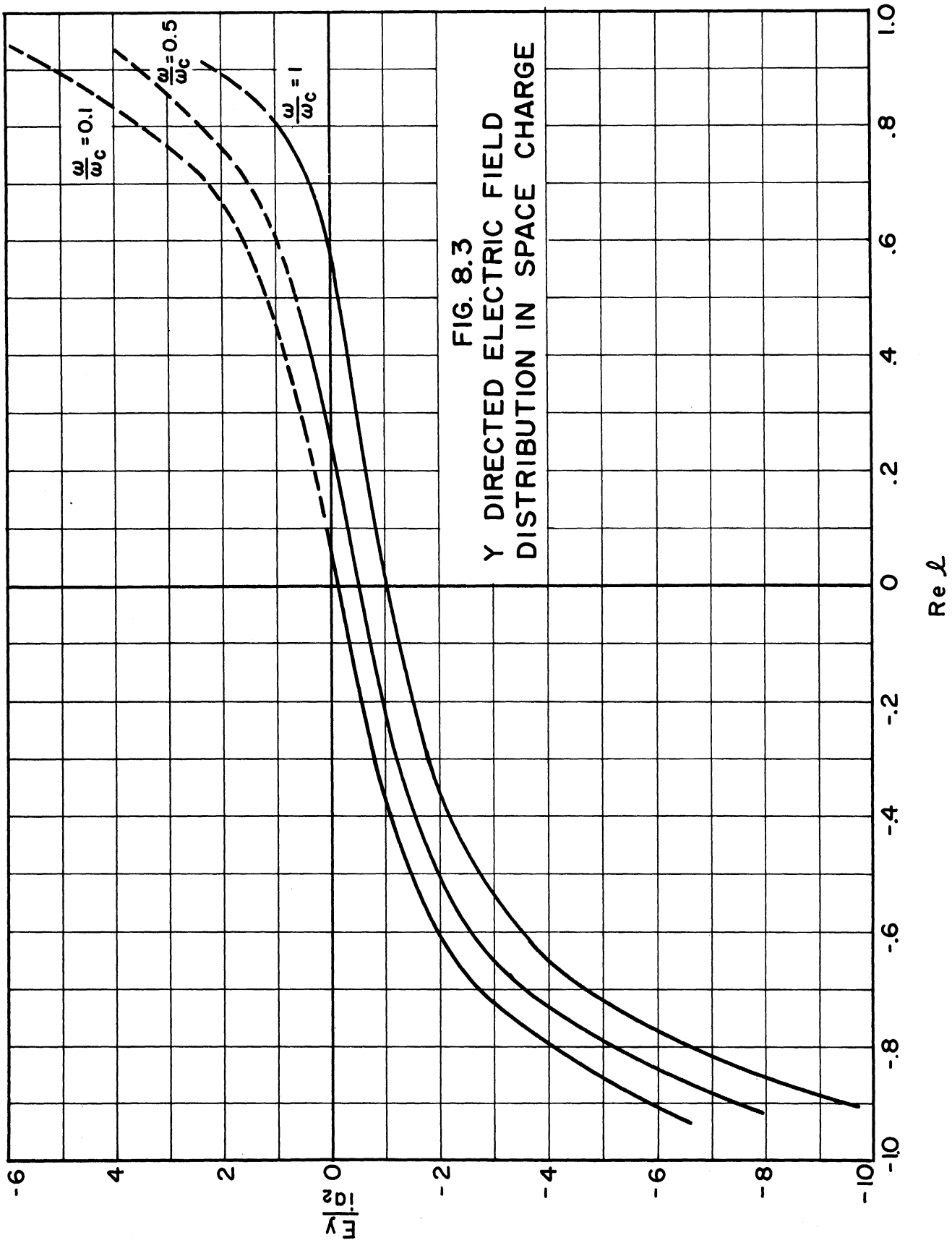
FIG. 8.3
Y DIRECTED ELECTRIC FIELD
DISTRIBUTION IN SPACE CHARGE
ω/ωc = 0.1
ω/ωc = 0.5
ω/ωc = 1
Ey/iα2
Re ℓ
-6
4
2
0
-2
-4
-6
-8
-10
1.0
.8
.6
.4
.2
0
-.2
-.4
-.6
-.8
-10

Using Eq 8-5, Eq 8-9 can be written in the form:

$$Y_e = \frac{H_z(h)}{E_x(h)} = \frac{ih\omega_c\epsilon_o}{\ell - \omega/\omega_c}\left\{\left[\omega/\omega_c - \frac{2\ell - \omega/\omega_c}{\ell^2}\right]\frac{1}{i}\frac{E_y(h)}{E_x(h)} + \frac{2\ell - \omega/\omega_c}{\ell^3}\right\}. \qquad (8\text{-}10)$$

In order to find an expression for the ratio $E_y(h)/E_x(h)$, $E_y(h)$ must be determined from the series solution for $E_x(h)$. From Eqs 8-3 and 8-8:

$$E_y(h) = i\frac{\partial E_x}{\partial \ell} = ia_2\left\{-\frac{\omega}{\omega_c}\left[1 + \frac{3}{2}\ell^2(h) + 1.05\,\ell^4(h) + \ldots..\right] + \left[2\ell(h) + 2\ell^3(h) + \ldots..\right]\right\}. \qquad (8\text{-}11)$$

This relation is plotted in Fig. 8.3. Therefore:

$$Y_e = \frac{E_y(h)}{E_x(h)} = i\,\frac{-\frac{\omega}{\omega_c}\left[1 + \frac{3}{2}\ell^2(h) + \ldots.\right] + \left[2\ell(h) + 2\ell^3(h) + \ldots.\right]}{-\frac{\omega}{\omega_c}\ell(h)\left[1 + \frac{1}{2}\ell^2(h) + \ldots.\right] + \ell^2(h)\left[1 + \frac{1}{2}\ell^2(h) + \ldots.\right]} \qquad (8\text{-}12)$$

Since the most interesting electron-wave interaction takes place when ℓ is small, i.e., when the electrons are near to synchronism with the travelling wave, it seems reasonable to neglect higher powers of $\ell(h)$ in Eq 8-12, which becomes:

$$\frac{E_y(h)}{E_x(h)} \cong i\,\frac{2\ell(h) - \frac{\omega}{\omega_c}}{-\frac{\omega}{\omega_c}\ell(h)}. \qquad (8\text{-}13)$$

Therefore the complete expression defining Y_e becomes [for small $\ell(h)$]:

$$Y_e = \frac{i\,\omega_c\,\epsilon_o\,h}{\ell\,(h) - \frac{\omega}{\omega_c}}\left[-2 + \frac{\omega/\omega_c}{\ell(h)} + \frac{4}{\frac{\omega}{\omega_c}\ell(h)} - \frac{2}{\ell^2(h)}\right]. \qquad (8\text{-}14)$$

It is seen that this equation for the electronic admittance possesses two singularities along the real axis of ℓ, one at Re $\ell = \omega/\omega_c$ and the other at Re $\ell = 0$. The former corresponds to the cathode and the latter to the synchronous layer of electrons. Also this equation shows the existence of two zeros of Y_e, one at Re $\ell = \frac{1}{2}\omega/\omega_c$ and the other at a large positive value of Re ℓ which is outside of the range of validity of Eq 8-14. This information is, of course, all contained in the curves of Figs. 8.2 and 8.3.

In order to determine the propagation characteristics of an electromagnetic wave propagating in the space charge, one must apply the boundary conditions imposed by the confining circuit. This can be expressed by letting $Y_e + Y_c = 0$, where Y_c is the admittance looking normally into the circuit. This work is continuing.

9. A Statistical Mechanical Study of the Steady-State Space-Charge Distribution in a Cutoff Magnetron (G. Hok)

A study of the steady-state space-charge distribution in a cutoff magnetron from the point of view of statistical mechanics has been concluded, although only qualitative results have been reached. A paper on the subject was read at the Electron Devices Conference in Durham, New Hampshire on June 22, 1951, and a technical report will be issued some time this summer.

Briefly, the results indicate that the interaction, however weak, between the discrete electrons in the space charge appreciably modify the steady state of the space charge from the distributions predicted by Brillouin, Slater, Page and Adams, Twiss, and others. Since a small current is always flowing, a thermal equilibrium is never established, but a steady state of diffusion is reached. The mathematical difficulties of even an approximate solution are very large, but some interesting conclusions can be drawn from

a qualitative discussion. The above will be presented in a technical report to be issued later.

10. Conclusions (J. R. Black)

The Model 9 magnetron has been operated both as a voltage-tunable device and as an oscillator in a mechanically tunable high-Q cavity. Problems relating to noise and power output are still present.

Cold tests on the Model 8 f-m magnetron, pertaining to the percentage of f-m modulation to be expected, are encouraging. A high-power c-w tube, employing two oscillator sections, is ready to be assembled. Power output of 1000 watts c-w is expected at 13-cm wavelength.

The study of the Model 6 f-m magnetron is being carried out by investigating the operation of the less complicated structure of the Model 7. This work has not progressed to the point where anything definite can be reported.

Study of propagation of electromagnetic waves in the magnetron space charge is essentially complete. A technical report is being prepared for publication in the near future.

The study of voltage-tuning and frequency-pushing phenomena is nearing completion. A technical report on this subject is expected to be published early this summer.

An analysis of the steady-state space-charge distribution in a cutoff magnetron has been completed and a technical report will be published soon.

The second model of the trajectron is ready for pumping and initial tests. This is a continuously-pumped model which can be taken down and reassembled readily. Magnetic materials such as Kovar have been eliminated

and it is hoped that difficulties experienced in the first model with beam alignment have been eliminated.

Technical Report No. 9 is in the process of being published and will be circulated soon. This report will contain several translated foreign articles which were of interest to the personnel of the Electron Tube Laboratory. It is hoped that this report will stimulate the circulation of articles translated at other laboratories.

11. Work in Prospect (J. R. Black)

Effort will continue to be directed towards the development of tubes. Work at a reduced rate will be continued on the trajectron. Technical reports will be published in the near future which will complete the theoretical studies which have been undertaken.

DISTRIBUTION LIST

22 copies — Director, Evans Signal Laboratory
Belmar, New Jersey
FOR - Chief, Thermionics Branch

12 copies — Chief, Bureau of Ships
Navy Department
Washington 25, D. C.
ATTENTION: Code 930A

12 copies — Director, Air Materiel Command
Wright Field
Dayton, Ohio
ATTENTION: Electron Tube Section

4 copies — Chief, Engineering and Technical Service
Office of the Chief Signal Officer
Washington 25, D. C.

2 copies — H. W. Welch, Jr., Research Physicist
Electron Tube Laboratory
Engineering Research Institute
University of Michigan
Ann Arbor, Michigan

1 copy — Engineering Research Institute File
University of Michigan
Ann Arbor, Michigan

W. E. Quinsey, Assistant to the Director
Engineering Research Institute
University of Michigan
Ann Arbor, Michigan

W. G. Dow, Professor
Department of Electrical Engineering
University of Michigan
Ann Arbor, Michigan

Gunnar Hok, Research Engineer
Engineering Research Institute
University of Michigan
Ann Arbor, Michigan

J. R. Black, Research Engineer
Engineering Research Institute
University of Michigan
Ann Arbor, Michigan

G. R. Brewer, Research Associate
Engineering Research Institute
University of Michigan
Ann Arbor, Michigan

J. S. Needle, Instructor
Department of Electrical Engineering
University of Michigan
Ann Arbor, Michigan

Department of Electrical Engineering
University of Minnesota
Minneapolis, Minnesota
ATTENTION: Professor W. G. Shepherd

Westinghouse Engineering Laboratories
Bloomfield, New Jersey
ATTENTION: Dr. J. H. Findlay

Columbia Radiation Laboratory
Columbia University
Department of Physics
New York 27, New York

Electron Tube Laboratory
Department of Electrical Engineering
University of Illinois
Urbana, Illinois

Department of Electrical Engineering
Stanford University
Stanford, California
ATTENTION: Dr. Karl Spangenberg

National Bureau of Standards Library
Room 203, Northwest Building
Washington 25, D. C.

Radio Corporation of America
RCA Laboratories Division
Princeton, New Jersey
ATTENTION: Mr. J. S. Donal, Jr.

Department of Electrical Engineering
The Pennsylvania State College
State College, Pennsylvania
ATTENTION: Professor A. H. Waynick

Document Office - Room 20B-221
Research Laboratory of Electronics
Massachusetts Institute of Technology
Cambridge 39, Massachusetts
ATTENTION: John H. Hewitt

Department of Electrical Engineering
Yale University
New Haven, Connecticut
ATTENTION: Dr. H. J. Reich

Department of Physics
Cornell University
Ithaca, New York
ATTENTION: Dr. L. P. Smith

Mrs. Marjorie L. Cox, Librarian
G-16, Littauer Center
Harvard University
Cambridge 38, Massachusetts

Mr. R. E. Harrell, Librarian
West Engineering Library
University of Michigan
Ann Arbor, Michigan

Mr. C. L. Cuccia
RCA Laboratories Division
Radio Corporation of America
Princeton, New Jersey

Dr. O. S. Duffendack, Director
Phillips Laboratories, Inc.
Irvington-on-Hudson, New York

Air Force Cambridge Research Laboratories
Library of Radiophysics Directorate
230 Albany Street
Cambridge, Massachusetts

Air Force Cambridge Research Laboratories
Library of Geophysics Directorate
230 Albany Street
Cambridge, Massachusetts
ATTENTION: Dr. E. W. Beth

Raytheon Manufacturing Company
Research Division
Waltham 54, Massachusetts
ATTENTION: W. M. Gottschalk

General Electric Research Laboratory
Schenectady, New York
ATTENTION: Dr. A. W. Hull

Missile and Radar Division
Raytheon Manufacturing Company
Waltham 54, Massachusetts
ATTENTION: Mr. James D. LeVan

Bell Telephone Laboratories
Murray Hill, New Jersey
ATTENTION: S. Millman

Special Development Group
Lancaster Engineering Section
Radio Corporation of America
RCA Victor Division
Lancaster, Pennsylvania
ATTENTION: Hans K. Jenny

Magnetron Development Laboratory
Power Tube Division
Raytheon Manufacturing Company
Waltham 54, Massachusetts
ATTENTION: Edward C. Dench

Vacuum Tube Department
Federal Telecommunication Laboratories, Inc.
500 Washington Avenue
Nutley 10, New Jersey
ATTENTION: A. K. Wing, Jr.

Microwave Research Laboratory
University of California
Berkeley, California
ATTENTION: Professor L. C. Marshall

General Electric Research Laboratory
Schenectady, New York
ATTENTION: P. H. Peters

Cruft Laboratory
Harvard University
Cambridge, Massachusetts
ATTENTION: Professor E. L. Chaffee

Research Laboratory of Electronics
Massachusetts Institute of Technology
Cambridge, Massachusetts
ATTENTION: Professor S. T. Martin

Collins Radio Company
Cedar Rapids, Iowa
ATTENTION: Robert M. Mitchell

Department of Electrical Engineering
University of Kentucky
Lexington, Kentucky
ATTENTION: Professor H. Alexander Romanowitz

Sperry Gyroscope Company
Library Division
Great Neck, Long Island, New York

2 copies — Mr. John Keto
Director, Aircraft Radiation Laboratory
Air Materiel Command
Wright Field
Dayton, Ohio